Geosci. Model Dev. Discuss., https://doi.org/10.5194/gmd-2017-169
Manuscript under review for journal Geosci. Model Dev.
Discussion started: 11 September 2017

Geoscientific Model Development Discussions

Coupling the Canadian Terrestrial Ecosystem Model (CTEM v. 2.0) to Environment and Climate Change Canada's greenhouse gas forecast model

Bakr Badawy[1,*], Saroja Polavarapu[1], Dylan B. A. Jones[2], Feng Deng[2], Michael Neish[1], Joe R. Melton[3], Ray Nassar[1], and Vivek K. Arora[3]

[1]Climate Research Division, Environment and Climate Change Canada, Toronto, Canada
[2]Department of Physics, University of Toronto, Toronto, Canada
[3]Climate Research Division, Environment and Climate Change Canada, Victoria, Canada
[*]Now at Faculty of Environment, University of Waterloo, Canada

Correspondence to: Bakr Badawy(bbadawy@uwaterloo.ca)

Abstract. The Canadian Land Surface Scheme and the Canadian Terrestrial Ecosystem Model (CLASS-CTEM) together form the land surface component in the family of Canadian Earth System Models (CanESM). Here, CLASS-CTEM is coupled to Environment and Climate Change Canada (ECCC)'s weather and greenhouse gas forecast model (GEM-MACH-GHG) to consistently model atmosphere-land exchange of CO_2. The coupling between the land and the atmospheric transport model ensures consistency between meteorological forcing of CO_2 fluxes and CO_2 transport. The procedure used to spin up carbon pools for CLASS-CTEM for multi-decadal simulations needed to be significantly altered to deal with the limited availability of consistent meteorological information from a constantly changing operational environment in the GEM-MACH-GHG model. Despite the limitations in the spin up procedure, the simulated fluxes obtained by driving the CLASS-CTEM model with meteorological forcing from GEM-MACH-GHG were comparable to those obtained from CLASS-CTEM when it is driven with standard meteorological forcing (CRU-NCEP). This is due to the similarity of the two meteorological datasets in terms of temperature and radiation. However notable discrepancies in the seasonal variation and spatial patterns of precipitation estimates, especially in the tropics, were reflected in the estimated carbon fluxes, as they significantly affected the magnitude of the vegetation productivity and, to a lesser extent, the seasonal variations in carbon fluxes. Nevertheless, the simulated fluxes based on the meteorological forcing from the GEM-MACH-GHG model are within the range of other estimates from bottom-up or top-down approaches. Indeed, when simulated fluxes obtained by driving the CLASS-CTEM model with meteorological data from the GEM-MACH-GHG model are used as prior estimates for an atmospheric CO_2 inversion analysis using the adjoint of the GEOS-Chem model, the retrieved CO_2 flux estimates are comparable to those obtained from other systems in terms of the global budget and the total flux estimates for the northern extratropical regions, which have good observational coverage. In data poor regions, as expected, differences in the retrieved fluxes due to the prior fluxes become apparent, but fall within the uncertainty bounds based on multi-inversion analyses. The coupling of CLASS-CTEM to an atmospheric transport model with carbon assimilation capabilities also provides insights into the limitations of CLASS-CTEM simulated CO_2 fluxes

Geosci. Model Dev. Discuss., https://doi.org/10.5194/gmd-2017-169
Manuscript under review for journal Geosci. Model Dev.
Discussion started: 11 September 2017

Geoscientific Model Development Discussions

through comparisons of simulated atmospheric CO_2 with observations at selected flask stations. This capability can be used to continually assess and improve the terrestrial ecosystem modules of the CLASS-CTEM model.

Copyright statement. TEXT

1 Introduction

Terrestrial ecosystems play a crucial role in the global climate-carbon system. Therefore, there is a need to better understand terrestrial biospheric processes related to the carbon cycle in order to obtain more reliable projections of their behavior under a changing climate. Given the great heterogeneity of vegetation and soils, the coverage and accuracy of the flux measurements are not sufficient for obtaining large-scale flux estimates with high confidence (Jung et al., 2009; Beer et al., 2010). As a result, considerable efforts have been made to develop terrestrial ecosystem models (TEMs) (whether simple regression or process-oriented) in order to quantify the magnitude, geographical distribution, and evolution of sources and sinks of carbon at regional and global scales (Potter et al., 1993; McGuire et al., 2001; Sitch et al., 2003; Thornton et al., 2005; Krinner et al., 2005; Reichstein et al., 2005; Badawy et al., 2013; Arora and Boer, 2005; Melton and Arora, 2016). However, systematic errors and uncertainties in the models can result from driving or forcing data (Jung et al., 2007; Clein et al., 2007; Zhao et al., 2006; Garnaud et al., 2014; Dalmonech et al., 2015; Anav et al., 2015; Wei et al., 2014), process formulation (also called model structure) (Sitch et al., 2015), model parameter specification, and initial conditions (Carvalhais et al., 2008, 2010; Melton et al., 2015; Zhu and Zhuang, 2015), leading to differing estimates of CO_2 fluxes from different models (McGuire et al., 2001; Piao et al., 2013; Sitch et al., 2015). Such differences in TEMs are among the main sources of uncertainty in future projections from coupled carbon-climate models (Anav et al., 2013; Friedlingstein et al., 2006; Arora et al., 2013; Friedlingstein et al., 2014). Therefore, there is a need to evaluate the performance of TEMs in order to identify and diagnose their weaknesses and strengths and ultimately reduce model uncertainties. Indeed, this is the motivation behind TEM multimodel intercomparisons efforts such as the Multi-scale Synthesis and Terrestrial Ecosystem Model Intercomparison Project (MsTMIP) (Huntzinger et al., 2013).

Inverse models (which relate concentrations to fluxes using an atmospheric transport model) are powerful tools to quantify carbon fluxes over large regions (Rödenbeck et al., 2003; Peters et al., 2007; Peylin et al., 2013) and can be used to evaluate the TEM results. However, inverse models suffer from deficiencies and uncertainties (Peylin et al., 2013) arising from transport errors, choice of observation network, observation uncertainties, and prior flux errors. Alternatively, there are carbon cycle data assimilation systems (CCDAS), which couple the strengths of the top-down (inversion) and bottom-up (i.e. TEM) approaches by embedding a TEM within a comprehensive climate model and using measurements from multiple streams to constrain the TEM (Scholze et al., 2003; Rayner et al., 2005; Koffi et al., 2013). The benefit is that biospheric models can then be validated on the global scale using atmospheric measurements of CO_2 that integrate the CO_2 signal at various spatial and temporal scales. Theoretically, in CCDAS, parameters of a TEM can also be optimized to improve its fit to atmospheric CO_2

Geosci. Model Dev. Discuss., https://doi.org/10.5194/gmd-2017-169
Manuscript under review for journal Geosci. Model Dev.
Discussion started: 11 September 2017

observations (Scholze et al., 2003; Rayner et al., 2005; Koffi et al., 2013; Kaminski et al., 2013), which can potentially yield greater understanding about underlying processes, and thus can help to improve the model performance.

Comprehensive Earth System Models need to include TEMs because the ecosystem responds to a changing climate. However, weather and carbon fluxes are also interconnected so that coupled weather and CO_2 prediction models operating on weather or seasonal timescales can also benefit from online TEMs. Specifically, if such a coupled model uses a prior flux estimate of terrestrial biosphere activity from an offline TEM, inconsistencies may arise when the TEM's meteorological driving data differs from that in the weather model. For example, at a given point in time, a TEM's grid cell might have experienced sunny weather and thus produced large CO_2 uptake whereas the weather model may indicate cloudy conditions and reduced CO_2 uptake. An online TEM constrained by the model's weather would have predicted this reduced CO_2. If such inconsistent CO_2 predictions are used to constrain inverse models there is a risk of misattributing some of the model-data mismatch to the flux estimate. Forecasting systems that integrate land and ocean CO_2 fluxes within numerical weather prediction (NWP) models have recently been developed (Agusti-Panareda et al., 2014; Ott et al., 2015) to produce short term predictions of atmospheric CO_2.

At Environment and Climate Change Canada (ECCC), a Carbon Assimilation System (EC-CAS) (Polavarapu et al., 2016) is being developed to assimilate satellite and in situ data to generate hindcasts of atmospheric CO_2 and estimates of regional fluxes of CO_2. A key objective of the work here is to assess the viability of land surface fluxes of CO_2 from the Canadian Terrestrial Ecosystem Model (CTEM) (Melton and Arora, 2014), coupled to the Canadian Land Surface Scheme (CLASS) (Verseghy, 2012), as a source of a priori biospheric fluxes of CO_2 for EC-CAS and other CO_2 flux inversion systems. EC-CAS is being created by adapting the operational weather prediction model GEM-MACH (Global Environmental Multi-scale - Modelling Air quality and CHemistry) (Moran et al., 2010; Robichaud and Ménard, 2014; Makar et al., 2015) for greenhouse gasses (called GEM-MACH-GHG hereafter, see Section 2.2). CLASS-CTEM is a process-based TEM which simulates the exchange of carbon, water and energy fluxes between the land surface and the atmosphere. It is similar in level of complexity to other TEMs (such as CASA (Potter et al., 1993) or SiB (Sellers et al., 1996)) which have been used for flux inversions and which have participated in multimodel intercomparisons such as that of Huntzinger et al. (2012). In recent studies (Melton and Arora, 2014; Melton et al., 2015; Melton and Arora, 2016; Badawy et al., 2016), CLASS-CTEM was calibrated based on observation-based climate data from the Climate Research Unit (CRU) (Harris et al., 2014) combined with reanalysis fields from the National Centers for Environmental Prediction (NCEP) (Kalnay et al., 1996).

Although incorporating CLASS-CTEM within EC-CAS is potentially mutually beneficial, the incorporation of a TEM designed for Earth System Modelling (decadal timescales) into a data assimilation system designed for short timescales (i.e. months to a few years) is not without its challenges. For example, the spin-up of carbon pools to present climate needs to be merged with the switch in climate data from reanalyses to that from the weather forecasting model (e.g. EC-CAS). The challenge is that operational weather forecasting systems are, by definition, constantly changing so that long archives of consistent analyses (i.e. with the same horizontal or vertical resolution or model coordinates or variable, etc.) are not available (see also Agusti-Panareda et al. (2016) for example), contrary to the case of reanalyses (e.g. ERA-Interim (Dee et al., 2011) or MERRA (Rienecker et al., 2011)). Given that the spin-up procedure is known to impact TEM predictions (Wutzler and Reichstein, 2007;

Geosci. Model Dev. Discuss., https://doi.org/10.5194/gmd-2017-169
Manuscript under review for journal Geosci. Model Dev.
Discussion started: 11 September 2017

Carvalhais et al., 2008, 2010), how will this affect the use of CLASS-CTEM in the flux estimation context? In addition, the environmental drivers of TEMs also impact their results, so will the change in the climate forcing of CLASS-CTEM negatively impact its predictions on these short "climate timescales"? Garnaud et al. (2014) show that carbon pools and fluxes from CLASS-CTEM are sensitive to climate datasets for the case of a limited area domain (North America). On the other hand, large changes in fluxes are not necessarily detectable by observing systems such as Greenhouse Gases Observing SATellite (GOSAT) (Ott et al., 2015) so such differences may not be perceptible in flux inversion results. Finally, given that there is already a well-documented sensitivity to prior flux estimates in data sparse regions (Gurney et al., 2004; Peylin et al., 2013), do such deficiencies in spin-up procedure and environmental drivers matter? In other words, despite the unavoidable imperfections in coupling a TEM from an Earth System Model to a Carbon Assimilation System focussed on short climate timescales, will the flux inversion results obtained using CTEM fall within the range of uncertainty encompassed by an ensemble of recognized flux inversion systems? The goal of this work is to answer these questions.

We begin in Section 2 with a description of the various models and datasets involved in this study, folowed by the experimental design (Section 3). In order to interpret differences in fluxes resulting from the change in meteorological forcing, we first compare the quality of the meteorological inputs from GEM-MACH-GHG against the standard climate forcing (CRU-NCEP) that was used to drive CLASS-CTEM, as well as against independent sources of data (Section 4.1). Then, we examine the sensitivity of the simulated carbon fluxes to the change in meteorological forcing to determine whether biases in the simulated carbon fluxes can be attributed to biases in the meteorological variables (Section 4.2). The simulated fluxes are assessed both directly as well as indirectly through their impact on CO_2 concentrations. Finally, in Section 4.3, the a priori fluxes from CTEM are used in a flux inversion system and the results are analyzed in terms of the seasonal cycle and annual totals of the optimized fluxes and the a posteriori CO_2 concentrations. The conclusions are presented in Section 5.

2 Models and Data

Before presenting the experimental design, we first introduce the TEM and the coupled meteorological and tracer transport model to which the TEM will be coupled. Then, CRU-NCEP and other datasets used to assess the various sources of climate forcing are described, followed by the experimental methodology.

2.1 CLASS-CTEM

The coupled CLASS-CTEM model used here is based on CLASS v3.6 (Verseghy, 2012) and an updated version of CTEM v1.2 (Melton and Arora, 2014) and runs globally on a Gaussian 128×64 grid that corresponds to $\sim 2.8^\circ \times 2.8^\circ$ grid spacing. CLASS calculates the biophysical exchange of energy and water fluxes between the land surface (soil, snow, and vegetation canopy) and the atmosphere. The model includes three soil layers, which extend to a total depth of 4.1 m, and one vegetation canopy and one snow layer. The model solves for the energy and hydrological balances at each grid cell using a half-hourly time step. The land surface of each grid cell is divided into four subareas: bare soil, vegetation, snow over bare soil and snow with vegetation. The vegetation within a grid cell, in CLASS, can be composed of 4 PFTs (Plant Functional Types): needleleaf trees,

Geosci. Model Dev. Discuss., https://doi.org/10.5194/gmd-2017-169
Manuscript under review for journal Geosci. Model Dev.
Discussion started: 11 September 2017

broadleaf trees, crops and grasses. For each PFT, prescribed physiological characteristics, such as albedo, annual maximum and minimum leaf area index (LAI), vegetation height, canopy mass, and rooting depth have to be specified. When coupled to CTEM, these structural vegetation attributes are dynamically simulated by CTEM with a daily time step and then passed to CLASS.

CTEM is a process-based terrestrial biosphere model that grows vegetation from bare ground and simulates the main processes governing carbon fluxes between the land biosphere and atmosphere. The model is parametrized and designed to simulate land-atmosphere exchanges of carbon through photosynthesis, ecosystem respiration (sum of autotrophic and heterotrophic respiration), phenology, turnover, mortality, allocation, fire and land use change (Arora, 2003; Arora and Boer, 2005; Melton and Arora, 2016). The model is represented by three living vegetation pools (leaves, stems, and roots) and two dead carbon pools (soil organic matter and litter). The terrestrial ecosystem processes are calculated for nine PFTs: Needleleaf evergreen, Needleleaf deciduous, broadleaf evergreen, broadleaf cold deciduous, broadleaf drought/dry deciduous, crops (C_3 and C_4) and grasses (C_3 and C_4). When coupled, CTEM provides time-varying vegetation structure attributes to CLASS and the calculated variables for the nine PFTs are averaged (weighted by the fractional coverage of each PFT) to obtain the four PFTs in CLASS that share similar functionality.

Within CTEM, photosynthesis and leaf respiration sub-modules operate on a half-hourly time step as in CLASS in order to model the effect of the CO_2 concentration on stomatal conductance. Other terrestrial ecosystem processes, including stem, root, and heterotrophic respiration are modelled at a daily time step. Recently, Badawy et al. (2016) modified CTEM to add the capability to simulate all respiratory fluxes at the same time step as CLASS (i.e. half-hourly) in order to model their diurnal variation caused by subdiurnal signals in the driving climate data. The current version of CTEM does not include the nitrogen cycle and its interactions with carbon cycle. Nevertheless, the model constrains the response of terrestrial photosynthesis to elevated CO_2 via an empirical formulation based on experimental plant growth studies (Arora et al., 2009). The model structure and its parametrizations are documented in Arora (2003), Arora and Boer (2005), and Melton and Arora (2016), in which a comprehensive description of model subroutines is provided.

Besides the meteorological inputs (shortwave and longwave downward radiation, air temperature, precipitation, specific humidity, surface pressure, wind speed (see Section 2.4)), the model requires data on soil texture (i.e. percentage of sand and clay for the three soil layers), fractional vegetation coverage for each PFT, organic matter content, permeable soil depth, and atmospheric CO_2. The soil texture information is based on Zobler (1986). The vegetation fractional coverage for the nine PFTs in CTEM are adapted from Arora and Boer (2010) but using the HYDE v3.1 data set for crop area (Hurtt et al., 2011) to reconstruct the historical land cover. The model uses inputs of annual mean atmospheric CO_2 concentrations, which are based on phase 5 of the Coupled model Intercomparison Project (CMIP5) (Meinshausen et al., 2011).

2.2 GEM-MACH-GHG

GEM-MACH is based on the dynamics and physics of the Global Environmental Multiscale (GEM) model (Côté et al., 1998a; Girard et al., 2013) at the Canadian Meteorological Centre (CMC). GEM is used for operational weather forecasting in both global and regional (North America) domains, whereas GEM-MACH includes an online chemical model that is fully integrated

Geosci. Model Dev. Discuss., https://doi.org/10.5194/gmd-2017-169
Manuscript under review for journal Geosci. Model Dev.
Discussion started: 11 September 2017

into the meteorological model to provide air quality forecasts over North America. GEM-MACH-GHG is a variant of GEM-MACH that removes the reactive chemistry and replaces it with climate-chemistry (e.g. OH climatology). In addition, a number of modifications to GEM-MACH were made, including the implementation of a mass conservation scheme, and modifying the vertical mixing in the boundary layer. A horizontal resolution of 0.9° (400×200 grid points), and a time step of 30 minutes are used.

In this study, the meteorological fields required to drive CLASS-CTEM are produced from GEM-MACH-GHG following the same approach as in Polavarapu et al. (2016) for the 2009-2010 period. Prior to 22 June 2009, the operational analyses were produced using a model with a lid at 10 hPa. Since that date, the operational model has used a much higher lid of 0.1 hPa and since the period of interest for greenhouse gas simulations commences with the launch of the Greenhouse Gases Observing Satellite (GOSAT) (Kuze et al., 2009; Yokota et al., 2009) in 2009, GEM-MACH-GHG uses the more recent model configuration. As a result, it is difficult to make use of CMC analyses prior to 22 June 2009. Thus, early in 2009, these analyses were supplemented by CMC archives of the "parallel run" (the system during its testing phase) and a preliminary run. Given that GEM-MACH-GHG was under development during this study, only a few years were simulated (2009-2010). There will always be an unsatisfactory length of analyses available for a TEM spin up period whenever operational weather forecast system is involved (e.g. Agusti-Panareda et al. (2016) also had similar issues). Moreover, greenhouse gas assimilation systems are constrained (by time, computational expense and the observing system) and thus often focus on a few years of study at one time (e.g Deng et al. (2014, 2016)). Thus, the challenge is to merge this small dataset into the spin-up procedure used for the TEM. As we shall see, despite this considerable challenge, the resulting impact on fluxes are still within the bounds of uncertainty provided by an ensemble of TEMs. The meteorological fields are initialized at the start of each 24h cycle with archived analyses from the CMC which were produced by the previously operational four-dimensional variational (4D-Var) data assimilation system (Charron et al., 2012), interpolated to GEM-MACH-GHG's 0.9° resolution. The 24-hour forecasts of shortwave and longwave radiation, surface temperature, wind speed, surface pressure, total precipitation, and specific humidity, were generated every 30 minutes, and then interpolated to the CLASS-CTEM grid.

2.3 GEOS-Chem

Previous inversion studies show that optimized fluxes are sensitive to prior fluxes particularly for regions that are poorly constrained by atmospheric observations such as the tropics (Peylin et al., 2013). In order to assess the quality of NEE from CTEM-GEM in comparison to other flux estimates, it is necessary to perform some inversion studies. Ideally, such inversions would be conducted with GEM-MACH-GHG but since the assimilation capability of EC-CAS is still under development, an alternative inversion system based on the GEOS-Chem model (http://geos-chem.org) is used. The GEOS-Chem model has often been used to simulate atmospheric CO_2 (e.g. Suntharalingam et al. (2004); Nassar et al. (2010)). This model is a global 3-D chemical transport model driven by assimilated meteorology from the Goddard Earth Observing System (GEOS-5) of the NASA Global Modelling and Assimilation Office (GMAO). Nassar et al. (2010) described an update of the atmospheric CO_2 simulation in GEOS-Chem. In this study, the model has a horizontal resolution of $4^\circ \times 5^\circ$, with 47 vertical layers from the surface to 0.01 hPa. The assimilation system is a 4D-Var data assimilation system in which a set of scaling factors is optimized

Geosci. Model Dev. Discuss., https://doi.org/10.5194/gmd-2017-169
Manuscript under review for journal Geosci. Model Dev.
Discussion started: 11 September 2017

to adjust the fluxes in each model grid box to better reproduce the observations over a given time period. In the 4D-Var system, the adjoint of the GEOS-Chem model is used to optimize the fluxes. Details of the GEOS-Chem adjoint model are given in Henze et al. (2007) and a description of its application for inverse modeling of atmospheric CO_2 is provided in Deng et al. (2014, 2016).

2.4 CRU-NCEP

The observation-based $0.5°$ monthly climatology from the Climate Research Unit (CRU, version TS3.2) (Harris et al., 2014) and the $\sim 2.5°$, 6-hourly reanalysis fields from the National Centers for Environmental Prediction (NCEP) (Kalnay et al., 1996) were combined to produce the CRU-NCEP global climate data set (Viovy, 2016) that has been described in Wei et al. (2014). The CRU-NCEP dataset provides globally gridded ($0.5° \times 0.5°$) 6-hourly time-varying climatology products that covers the period 1901-2014. The input data from CRU-NCEP includes shortwave and longwave radiation, surface temperature, wind speed, surface pressure, total precipitation, and specific humidity. These climate data were interpolated to the CLASS-CTEM's grid and disaggregated to a half-hourly time step as described in Arora and Boer (2005), and Melton and Arora (2014).

2.5 Other Datasets

To evaluate the quality of the GEM driving data, the forecasted fields of shortwave radiation, temperature, and precipitation for 2009 and 2010 are compared with CRU-NCEP, and both are evaluated against the CRU dataset and the ERA-Interim reanalysis (hereafter called ERAI) of the European Centre for Medium-Range Weather Forecasts (ECMWF)(Berrisford et al., 2011; Dee et al., 2011). The $2.5°$ monthly ERAI data is available at the ECMWF data server.

To assess the impact of using alternative driving data on the simulated fluxes, the CLASS-CTEM fluxes obtained with GEM and CRU-NCEP meteorology are compared and evaluated against independent observation-based flux estimates and other model results. For example, the simulated GPP was compared with the observation-based estimates of gross primary productivity (GPP) produced by Beer et al. (2010) (called B10 hereafter). They are based on eddy covariance flux data and several data-driven models, and averaged for the period 1998 to 2005. The model results are also compared with the multi-year average 3-hourly GPP and ecosystem respiration (R_{eco}) from the Boreal Ecosystem Productivity Simulator (BEPS) (Chen et al., 2012), in which the annual terrestrial ecosystem exchange imposed in each grid box ($4° \times 5°$) is neutral (Deng and Chen, 2011) (i.e. GPP = R_{eco}). BEPS is driven by NCEP reanalysis dataset. Finally, the model results are evaluated using the a posteriori CO_2 fluxes from the CarbonTracker data assimilation system (Peters et al., 2007) (version CT2013B) available at http://carbontracker.noaa.gov. All datasets used in evaluating the model's results are re-gridded to the CLASS-CTEM grid.

We evaluate the results of the inversion analyses (described in section 3.3) using the GEOS-Chem model by comparing the a posteriori CO_2 fields to atmospheric CO_2 observations from the Total Carbon Column Observing Network (TCCON) from which the column-averaged dry-air mole fractions of CO_2 (XCO2) are retrieved (Wunch et al., 2011). TCCON data were obtained from the TCCON Data Archive, hosted by the Carbon Dioxide Information Analysis Center (CDIAC) (http://tccon.ornl.gov/). For the comparisons, we use observations from the current TCCON GGG2014 data set from 13 different sites (Table 1) (see also Deng et al. (2014)) in 2009 and 2010. We also evaluate the inversion analyses using aircraft data from

Geosci. Model Dev. Discuss., https://doi.org/10.5194/gmd-2017-169
Manuscript under review for journal Geosci. Model Dev.
Discussion started: 11 September 2017

the HIAPER Pole-to-Pole Observations (HIPPO) project (http://hippo.ornl.gov/). We use the 10-second averaged data from the HIPPO-1, HIPPO-2, HIPPO-3 campaigns (Wofsy, 2011; Wofsy et al., 2012), for 9 to 21 January 2009, 31 October to 22 November 2009, and 24 March to 16 April 2010, respectively.

3 Experimental Design

When coupling CLASS-CTEM to EC-CAS, we first identify a necessarily-imperfect spin-up procedure that transitions from climate data forcing from a standard dataset such as CRU-NCEP to a short sequence of operational meteorological analyses (Section 3.1). Once fluxes are available from CLASS-CTEM for CRU-NCEP meteorology with the standard spin-up procedure and from GEM-MACH-GHG with the modified spin-up procedure, the simulations of CO_2 that are performed with GEM-MACH-GHG are described in Section 3.2. Finally, the a priori fluxes from CLASS-CTEM are tested in a flux inversion experiment which is described in Section 3.3.

3.1 CLASS-CTEM Runs

To test the sensitivity of the simulated carbon fluxes to the meteorological forcing, we performed a series of experiments with CLASS-CTEM using two different meteorological inputs from (1) CRU-NCEP (hereafter called CTEM-CRUNCEP), which has been used to drive CLASS-CTEM simulations in previous studies (Melton and Arora, 2014; Melton et al., 2015; Badawy et al., 2016), and (2) GEM-MACH-GHG (hereafter called CTEM-GEM). For the CTEM-CRUNCEP run, the model was first initialized (to represent the pre-industrial period 1861-1900) by running it to equilibrium using repeated 1901-1940 CRU-NCEP climate, a constant globally uniform CO_2 of 286.37 ppm, and a fixed vegetation fractional coverage corresponding to the year 1861 until carbon pools and fluxes were in steady state (zero mean annual net ecosystem exchange (NEE)). The model was then run from 1901-2010 using varying CO_2 concentrations and CRU-NCEP meteorology.

For the CTEM-GEM run, the meteorological inputs from GEM-MACH-GHG were only available for 2009-2010 at the time of this study, and hence no global climate data available for the pre-industrial run. In general, reanalysis output begins around 1949 (e.g. NCEP-NCAR reanalyses) when the observing system had sufficient coverage, and as noted earlier, analyses from operational systems are restricted to much shorter and recent periods because of the constant change in model, observations and assimilation schemes. Therefore, the spin-up simulation was performed with a constant uniform CO_2 concentration of 387.4 ppm (corresponding to 2009) and a fixed vegetation fractional coverage corresponding to the same year. The spin-up simulations were driven with repeated meteorological data for the 2009-2010 period until model pools reached equilibrium. The transient simulation for the 2009-2010 period was then initialized from the spin-up simulations using varying CO_2 concentrations and GEM meteorology.

To assess the impact of using present climate to spin up the model on the simulated carbon pools and fluxes, we also performed a special run that used repeated meteorological data for 2009-2010 from CRU-NCEP, and constant uniform CO_2 of 387.4 ppm, and a fixed vegetation fractional coverage corresponding to the year 2009 until the model pools reach equilibrium (hereafter CTEM-CRUNCEP2yr).

Geosci. Model Dev. Discuss., https://doi.org/10.5194/gmd-2017-169
Manuscript under review for journal Geosci. Model Dev.
Discussion started: 11 September 2017

Note that fire and land use change are not taken into account in the current model's simulations due to the large uncertainty in the global land use history (Houghton et al., 2012) that may yield significant biases in the simulated CO_2 fluxes. Also, the standard model parameters were not changed or tuned to improve model performance when using alternative meteorological inputs. Hence the main differences between the CLASS-CTEM runs are the meteorological inputs, and the set-up of the spin-up simulations.

3.2 Forward simulation using GEM-MACH-GHG model

Forward simulations are performed using the GEM-MACH-GHG model to evaluate how well CLASS-CTEM, using meteorological inputs from GEM-MACH-GHG, is able to reproduce temporal variations in atmospheric CO_2 at monitoring stations. The estimated NEE from CTEM-CRUNCEP and CTEM-GEM were used as a surface boundary condition in GEM-MACH-GHG, which transports the signal from the surface fluxes throughout the atmosphere, to validate the resulting modelled concentrations against observations of atmospheric CO_2. The other fluxes are kept the same as in Polavarapu et al. (2016). Specifically, the anthropogenic emissions from fossil fuel burning and cement manufacturing, biomass burning, ocean-atmosphere carbon exchange and initial atmospheric concentration (Jan 1, 2009) are based on CT2013B (Peters et al., 2007).

3.3 Inversion Analysis Configuration in the GEOS-Chem Model

Because flux inversions have been performed for over a decade with the in situ measurements, there is a considerable body of literature of such inversion results (e.g. Rödenbeck et al. (2003); Peters et al. (2007), and Peylin et al. (2013)). Consequently, for our experiments, we use this observing network as opposed to a combined one that includes the more recent satellite missions. Thus, the GEOS-Chem flux inversions use the flask observations of atmospheric CO_2 collected by NOAA ESRL Carbon Cycle Cooperative Global Air Sampling Network sites (Dlugokencky et al., 2015) and ECCC sampling sites (Worthy et al., 2009). We use the same set of observation sites as described in Deng et al. (2014) (see their Section 2.1.2).

In this study, we use the similar a priori CO_2 fluxes of the anthropogenic emissions from fossil fuel burning and cement manufacturing, biomass burning, and ocean-atmosphere carbon exchange described in Deng et al. (2014) in order to maximize comparability with the those results. However, for the biospheric flux of CO_2, we conducted three runs using three different NEE priors from CTEM-GEM, CTEM-CRUNCEP, and BEPS. The optimized 3-D CO_2 mixing ratio field from CarbonTracker was used as the initial CO_2 field in the inversion runs.

4 Results and Discussion

For the meteorological data, we compare temperature, shortwave radiation, and precipitation, which are considered to be the most important variables controlling land carbon dynamics (Piao et al., 2013). We also compare the component fluxes of GPP, R_{eco}, and net ecosystem exchange (NEE = R_{eco} - GPP) in order to identify the potential drivers of differences between model simulations. To examine regional differences, data and model output are also spatially aggregated to the 11 land regions of the TransCom inverse model inter-comparison project (Gurney et al., 2003).

Geosci. Model Dev. Discuss., https://doi.org/10.5194/gmd-2017-169
Manuscript under review for journal Geosci. Model Dev.
Discussion started: 11 September 2017

4.1 Differences in Meteorological Forcing

Here, we evaluate the meteorological data from GEM by comparing it against CRU-NCEP, CRU and ERAI datasets where possible. Figure 1 shows the spatial patterns of the differences in mean annual temperature between GEM, CRU-NCEP, and CRU for 2009 and 2010. The differences between CRU-NCEP and CRU show cold biases in middle and high Northern latitudes and warm biases in Africa and South America. CRU-NCEP retains the monthly climatology of CRU but adds the daily and diurnal variations of NCEP reanalyses (Wei et al., 2014). Thus differences in annual mean temperature of CRU and CRU-NCEP should be small by design. In contrast, GEM is warmer than CRU over the North high latitudes and generally cooler elsewhere. The comparison also shows that CRU-NCEP is cooler than GEM in Northeastern North America, Eastern Europe, and Eastern Asia, and warmer in Africa, Southwestern Asia, South America, and the west coastline of North America. The differences in Figs. 1e and 1f are much larger than those seen in Figs. 1a and 1b because GEM analyses are completely independent of CRU. NCEP reanalyses are constrained by the global meteorological observing system and the datasets used in 2009-2010 are likely broadly similar to that used by operational centers such as ECCC. Indeed, Zhao et al. (2006) compared meteorological fields from NCEP, the Data Assimilation Office (DAO) (currently called the GMAO), and ECMWF for the 2000-2003 period and found that the NCEP fields had a cold bias at all latitudes and that the bias was largest in the tropics, which is similar to the bias in the GEM fields. Zhao et al. (2006) also found that the ECMWF ERA-40 (the precursor to ERAI) and DAO fields had smaller zonal mean biases compared to NCEP, but the ERA-40 fields were similar to those from GEM in that they had a high bias at high latitudes.

To better illustrate the differences between the datasets, we have plotted in Fig. 2 the monthly mean temperature averaged for the 11 TransCom land regions. All the data show the same seasonal variations, with opposite phases of temperature between hemispheres. The largest differences are found in the tropics and the Southern hemisphere. GEM tends to be biased low compared to the other data in Northern Africa, Southern Africa and temperate South America. CRU-NCEP overall is in better agreement with the observations (CRU). This is not surprising given that CRU-NCEP was produced by combining CRU and NCEP/NCAR Reanalysis products.

Figure 3 shows the spatial distribution of the differences of mean annual shortwave radiation between GEM and CRU-NCEP, and ERAI datasets for 2009 and 2010. Shortwave radiation estimates are not available in the CRU data set. The comparison indicates that CRU-NCEP is approximately 15-70 W m^{-2} higher (sunny bias) than ERAI in the high latitudes and in the tropical land regions. In arid areas (i.e. Australia, Sahara, South Africa, Southern North America, Tibetan Plateau, and West Asia), CRU-NCEP is approximately 15-50 W m^{-2} lower than ERAI. In contrast, GEM is approximately 10-60 W m^{-2} higher than ERAI over all land regions, with the highest values (40-60 W m^{-2}) over tropical lands. The shortwave radiation estimates from GEM is approximately 10-80 W m^{-2} higher than those from CRU-NCEP over nearly all land regions, with the exception of Europe, Eastern North America and in a few grid cells in the tropical regions, where CRU-NCEP is higher (10-80 W m^{-2}).

Figure 4 shows the monthly mean shortwave radiation averaged for the TransCom land regions. GEM and ERAI have more similar seasonal variability compared to CRU-NCEP in most of the land regions, especially in in the tropics. However, ERAI shows slightly lower monthly mean values in Eurasia regions, and in tropical South America. Zhao et al. (2006) also found

Geosci. Model Dev. Discuss., https://doi.org/10.5194/gmd-2017-169
Manuscript under review for journal Geosci. Model Dev.
Discussion started: 11 September 2017

that ERA-40 (the precursor to ERAI) underestimated shortwave radiation in the tropics. Differences between the datasets in the tropics may be due to cloudiness biases over the Intertropical Convergence Zone (ITCZ) region, which have a large impact on radiative forcing (Dee et al., 2011).

The comparisons of the differences in annual total precipitation between GEM, CRU-NCEP, and CRU datasets are shown in Fig. 5. The smallest differences are between CRU-NCEP and CRU. The largest differences in magnitude between CRU-NCEP and CRU are mainly in the tropics, particularly tropical Asia, and along the west coast of South America. Also, the largest differences between GEM and CRU are in the tropics. The comparison also indicates that CRU-NCEP is wetter than GEM in the tropics and sub-tropics, and in the temperate regions, but is drier than GEM in some areas of the boreal regions, and over a few grid cells in central Africa, and China. In general, the tropics exhibit the largest differences between the GEM and CRU-NCEP datasets.

The comparisons between the monthly total precipitation integrated over the TransCom land regions are shown in Fig. 6. Unlike temperature and shortwave radiation (well represented by global models), there is a very clear difference in monthly total precipitation among the datasets, except between CRU-NCEP and CRU, which agree very well with some differences in the tropics. It is clear that the largest differences occur mainly during summer in each hemisphere, which is associated with high precipitation. GEM tends to be drier mainly during summer. Despite the differences in the seasonal amplitude, GEM shows a quite similar seasonal variability compared to other datasets. We should keep in mind that precipitation estimates from the reanalysis/forecast systems are normally associated with large errors (Harris et al., 2014), particularly over land. These errors are due to problems with the convective parametrization in the models, and the fact that ground-based precipitation observations are not yet used in the data assimilation systems. On the other hand, CRU monthly precipitation suffers large biases in areas where observations are sparse (i.e. tropics and southern Hemisphere) (Harris et al., 2014). In fact, the observation-based datasets are not based only on measurements, but are also sometimes model-dependent (i.e. filling gaps, interpolation, etc) (Harris et al., 2014). These deficiencies as well as the different spatial/temporal resolutions among models and observations can explain some of the differences between the datasets. Deficiencies in ERAI and CRU have been investigated in previous studies (Simmons et al., 2010; Balsamo et al., 2010; Szczypta et al., 2011).

In summary, the meteorological fields from GEM are similar in quality to those from reanalyses (ERAI) and observation-based (CRU and CRU-NCEP) datasets. However, there are some notable discrepancies in seasonal variations and spatial distribution patterns between GEM and CRU-NCEP, particularly in precipitation estimates in the tropics, which will be reflected in the estimated carbon fluxes. Biases in precipitation may indicate that the convective scheme used in GEM system needs to be improved, in particular, over the tropics. CLASS-CTEM driven by GEM precipitation will be impacted by these biases.

4.2 Impact of Meteorological Forcing on Carbon Fluxes

Here, we assess the impact of changing meteorological inputs on the simulated carbon fluxes to determine whether biases in fluxes can be attributed to biases in the meteorological variables.

Geosci. Model Dev. Discuss., https://doi.org/10.5194/gmd-2017-169
Manuscript under review for journal Geosci. Model Dev.
Discussion started: 11 September 2017

4.2.1 Differences in Simulated Carbon Fluxes

To evaluate the spin-up procedure, the simulated global values of primary carbon pools and fluxes are summarized in Table 2 for the spin-up simulations from CTEM-CRUNCEP (which used the 1901-1940 climate data for the spin-up), and CTEM-GEM (which used the 2009-2010 climate data for the spin-up). CTEM-GEM produces smaller values of carbon pools and fluxes compared to CTEM-CRUNCEP. One possible explanation for this is the use of the present climate to spin up the model in the case of CTEM-GEM. Table 2 shows also the global values of carbon pools and fluxes simulated by the CTEM-CRUNCEP2yr experiment, which also uses just the 2009-2010 climate to spin up the model. Rather than reducing the size of carbon pools, CTEM-CRUNCEP2yr produces much higher values compared to both CTEM-CRUNCEP and CTEM-GEM. Table 2 also compares the mean areal land precipitation globally as well as for the tropical land band (30°N-30°S) averaged over the 1901-1940 (for CTEM-CRUNCEP), and 2009-2010 (for CTEM-CRUNCEP2yr and CTEM-GEM). For the CRU-NCEP runs, 2009-2010 is wetter than the 1901-1940 period at global and tropical scales, which can explain the higher productivity in CTEM-CRUNCEP2yr compared to CTEM-CRUNCEP. On the other hand, GEM precipitation (2009-2010) is slightly higher than CRU-NCEP (1901-1940) at the global scale, but lower over the tropical band for the same periods. The drier tropical band is reflected in the estimated tropical GPP from CTEM-GEM (Table 2), which dominates the global total GPP (Beer et al. (2010), Anav et al. (2015), and many others). This may explain the low carbon pools simulated by CTEM-GEM. This comparison suggests that precipitation plays a significant role in plant productivity in the tropics, and thus accurate precipitation patterns are necessary to establish realistic initial values for carbon pools and fluxes during the spin-up runs. Despite the differences in model inputs and spin-up configuration, the initial global carbon pools and fluxes from CTEM-GEM, however, are still within the range of the other estimates (Melton and Arora, 2014, Table 2).

The low GPP values from CTEM-GEM warrant further discussion given that the initial estimates of carbon pools and fluxes are critical to obtain an accurate estimate of historical CO_2 fluxes (Exbrayat et al., 2014; Tian et al., 2015). Carbon stocks are often not well modeled in TEMs (Houghton et al., 2012; Tian et al., 2015). The modeled pool sizes can be adjusted by tuning the model parameters in order to match observation-based estimates of carbon stocks. For example, Carvalhais et al. (2008, 2010) have reported the limitation of the carbon cycle steady state assumption in TEMs. Carvalhais et al. (2010), therefore, introduced a new parameter in the CASA model that forced the adjustment of both vegetation and soil carbon pools from equilibrium (after spin-up) allowing for model runs to be initialized either as net sinks or sources. They found that including this new parameter yielded better model performance in simulating carbon fluxes in comparison to observations. Moreover, their modeled soil carbon stocks became closer to observations. However, large uncertainties and errors in measurements can produce biased parameters, and hence poor model performance. Thus, forcing agreement to a given global mean value of GPP (e.g. 120 Pg C/yr) by tuning model parameters may lead to worse model performance and is not justifiable given the observational uncertainty in this value. Given that CLASS-CTEM will provide only a prior estimate of NEE (at least in the first stage) for flux inversions in EC-CAS, adjusting the initial carbon pools modeled by CLASS-CTEM is not necessary and would not likely change the major conclusions derived here. Moreover, tuning of CLASS-CTEM specifically for the far-from-ideal spin-up process that we employed for the GEM fields would be dubious and would make comparison with CTEM-CRUNCEP

Geosci. Model Dev. Discuss., https://doi.org/10.5194/gmd-2017-169
Manuscript under review for journal Geosci. Model Dev.
Discussion started: 11 September 2017

results difficult. Beyond the global budget, which is well constrained by atmospheric data (Peylin et al., 2013), the main focus is to assess the ability of the model to simulate the spatial and temporal flux variations in response to changes in environmental conditions and its ability to match the atmospheric signal.

For transient simulations, the simulated terrestrial carbon fluxes for 2009-2010 from the two simulations (CTEM-CRUNCEP and CTEM-GEM) are compared to each other as well as to observation-based estimates (where possible) or independent model results. Figure 7 shows the annual spatial difference of GPP simulated by CLASS-CTEM (2009-2010) and the observation-based GPP estimates from B10 (averaged over the period 1998 to 2005). The figure also shows the spatial difference between the modeled GPP from BEPS and B10 and the zonal distribution of GPP from all datasets. There are significant differences in the annual GPP between the two simulations (CTEM-CRUNCEP and CTEM-GEM) and the evaluation data, particularly in the most highly vegetated areas (i.e. the tropics, and the boreal and temperate regions). CTEM-CRUNCEP and CTEM-GEM have similar spatial differences over Western Europe and boreal Asia, and to a lesser extent over North America but they show poor agreement in the tropics. Tropical GPP from CTEM-CRUNCEP is overestimated compared to B10. In contrast, it is underestimated in the Amazonian region, western Africa, and tropical Asia with CTEM-GEM. In comparison to other model results, the spatial distribution of the difference between BEPS and B10 (Fig. 7a) reveals different patterns almost everywhere. The zonally averaged GPP in Fig. 7b indicates that CTEM-CRUNCEP and BEPS agrees very well with B10 compared to CTEM-GEM, which underestimate GPP over the tropics.

Since the formulation of most models, including CLASS-CTEM and BEPS, links respiration to photosynthesis (Melton and Arora, 2016), R_{eco} estimates from both simulations and BEPS show a similar pattern to GPP (spatially and zonally), with significant differences in the most productive ecosystems (not shown here). The large discrepancies in seasonal variations and spatial distribution patterns between GEM and CRU-NCEP are due to the precipitation differences (temperature and shortwave radiation have much better agreement), particularly in the tropics. Figures 5 and 7 suggest that the differences in the spatial pattern of GPP are more closely associated with precipitation than temperature or shortwave radiation differences over the tropics. This is consistent with previous findings (Nemani et al., 2003; Jung et al., 2007; Beer et al., 2010; Piao et al., 2013; Anav et al., 2015) that interannual variation of productivity is primarily correlated with the precipitation over the tropics.

To examine regional differences, the seasonal variation and the annual mean of GPP from both simulations, and BEPS are also spatially aggregated to the 11 TransCom land regions in Fig. 8. For R_{eco} (not shown here), the same conclusions can be drawn as from the GPP figures. Figure 8 shows that the seasonal variations of GPP from CTEM-CRUNCEP are consistently higher than those from CTEM-GEM. In the northern hemisphere regions, flux estimates have large seasonal variations, i.e., small values in winter and high values in summer, reflecting the seasonal change in carbon uptake by the land vegetation. The largest differences between CTEM-CRUNCEP and CTEM-GEM, in terms of the amplitude of the seasonal cycle, are found in the tropics, with CTEM-GEM having smaller amplitudes. However, in tropical Asia, the seasonal cycle from CTEM-GEM agrees well with BEPS compared to CTEM-CRUNCEP, which has larger annual GPP and R_{eco} (not shown here). In general, CTEM-GEM have some differences compared to CTEM-CRUNCEP over all regions mainly in terms of the amplitude, and to a lesser extent in the phase of the seasonal cycle. This is consistent with the findings of Dalmonech et al. (2015) who tested the impact of coupled and uncoupled configurations of JSBACH land surface component of the Max Planck Institute Earth System

Geosci. Model Dev. Discuss., https://doi.org/10.5194/gmd-2017-169
Manuscript under review for journal Geosci. Model Dev.
Discussion started: 11 September 2017

Model (MPI-ESM) on the simulated land carbon fluxes. They found that biases in the meteorological forcing to a large extent control the magnitude of GPP rather than the phenology and seasonal cycle of productivity, which could be more related to the model formulations (i.e. the timing and length of the growing season).

The annual GPP, R_{eco}, and the net flux are given in Table 3. Annual GPP values from CTEM-GEM for 2009 and 2010 are smaller than the multi-year average of GPP from BEPS (119.5 Pg C) (Deng et al., 2014), and from B10 (123 ± 8 Pg C). On the other hand, annual GPP values from CTEM-CRUNCEP for 2009 and 2010 are higher than those from BEPS and B10. This leads to a stronger land carbon sink from CTEM-CRUNNCEP compared to CTEM-GEM (Table 3). The weaker sink in CTEM-GEM is due to the lower precipitation estimates in the tropics (the region that mainly controls interannual variability in the carbon cycle), and hence lower global GPP (Piao et al., 2013; Beer et al., 2010).

To assess the impact of the differences in GPP and R_{eco} from CTEM-CRUNCEP and CTEM-GEM on the seasonal cycle of NEE (the difference between GPP and R_{eco}), Fig. 9 compares the NEE seasonal cycle from both simulations with the simulated prior NEE from BEPS (multi-year average) and the optimized NEE from CT2013B for 2009 and 2010 over the TransCom land regions. BEPS produces the smallest amplitude of the seasonal cycle of NEE while CTEM-CRUNCEP has the largest amplitude in northern land regions, except boreal Eurasia where the optimized NEE from CT2013B exhibits the largest amplitude (Fig. 9). For the South American tropical region, all models show considerable disagreement in the seasonal cycle, sometimes with opposite phases. In the northern hemisphere, CTEM-GEM and CTEM-CRUNCEP have better agreement with each other during winter than in summer. CTEM-GEM also tends to have the peak of the growing season one month earlier than CTEM-CRUNCEP (i.e. Eurasian boreal and North America temperate) due to the differences in GPP seasonal cycle (see Fig. 8). Even though there is large difference in the amplitude of the seasonal cycle of GPP (the same for R_{eco} - not shown here) from CTEM-GEM compared to CTEM-CRUNCEP (Fig. 8), the difference is much smaller in NEE. This is due to the fact that NEE is the difference between two large terms (GPP and R_{eco}). That means, even though GPP and R_{eco} have large biases compared to observation-based estimates, the biases in NEE are much smaller.

Despite the significant differences in model inputs, and differences in model structure and methods, the CTEM-GEM flux estimates are within the range of the other estimates from TEMs used as a priori estimates in flux inversions (i.e. BEPS) or measurement-constrained fluxes (i.e. CT2013B). Accordingly, the prior information from CTEM-GEM is considered to be suitable for testing in the data assimilation context. However, flux estimates in the tropics from CTEM-GEM should be treated with caution.

4.2.2 Modelled CO_2 Concentration

To assess the quality of the CO_2 fluxes from CLASS-CTEM simulations, terrestrial NEE fluxes from CTEM-CRUNCEP and CTEM-GEM are used as a priori land fluxes in the GEM-MACH-GHG global atmospheric CO_2 transport model. For comparisons, GEM-MACH-GHG was also run using the posterior NEE fluxes from CT2013B as described in Polavarapu et al. (2016). In these forward simulations, the anthropogenic emissions from fossil fuel burning and cement manufacturing, biomass burning, ocean-atmosphere carbon exchange are based on CT2013B (Peters et al., 2007) so that the only difference between the three runs is the terrestrial NEE fluxes.

Geosci. Model Dev. Discuss., https://doi.org/10.5194/gmd-2017-169
Manuscript under review for journal Geosci. Model Dev.
Discussion started: 11 September 2017

Figure 10 compares the modeled CO_2 time series from the two CLASS-CTEM simulations with that based on the CT2013B posterior fluxes, and with observed CO_2 at Alert Bay, Canada (82.45°N, 62.52°W) and Mauna Loa, Hawaii (19.53°N, 155.58°W) (Worthy et al., 2009; Dlugokencky et al., 2015). At both observation sites, the simulations forced with CTEM-CRUNCEP and CTEM-GEM NEE fluxes (red and blue curves) have a similar overestimation of the observed atmospheric CO_2 from December to June, but the simulation forced with CT2013B fluxes (green curves) has a much better match to observations. This makes sense because CT2013B fluxes have been informed by atmospheric observations whereas the other two fluxes have not. The differences between the modeled and observed CO_2 might also indicate deficiencies in the seasonal cycle of flux estimates from CTEM-CRUNCEP and CTEM-GEM. Interestingly, for Alert, the simulation forced with CTEM-GEM has a better match to observations during the autumn of both years compared to those driven by CTEM-CRUNCEP and CT2013B, which underestimate atmospheric CO_2. As explained in Polavarapu et al. (2016), the autumn underestimation at Alert with CT2013B fluxes is likely due to a mismatch in seasonal-scale meridional transport between GEM-MACH-GHG and TM5 (the model used to produce CT2013B). For Mauna Loa, CTEM-GEM has worse agreement with the observations, especially during winter. The overestimation of atmospheric CO_2 at Mauna Loa with CTEM-GEM is likely due to the less net uptake over the tropics as discussed before.

Figure 11 shows the zonal mean CO_2 for the 3 simulations (CTEM-CRUNCEP, CTEM-GEM, and CT2013B) for selected winter and summer dates. In general, the zonal mean fields from the three simulations have good agreement in the upper levels with the greatest differences near the surface. In winter, the CTEM-GEM simulation (center panels) produces high net emission (less carbon uptake) over the northern hemisphere, while CTEM-CRUNCEP (left panels) and CT2013B (right panels) show quite similar zonal means. In summer the CTEM-CRUNCEP simulation shows higher CO_2 over the northern hemisphere compared to CTEM-GEM and CT2013B, which have better agreement but to a lesser extent in summer 2010.

Overall, the comparison reveals that the modelled CO_2, at Alert and Mauna Loa, from both CTEM-CRUNCEP and CTEM-GEM are generally in agreement, despite the differences in the meteorological inputs and the spin-up approach. Thus, despite the imperfect TEM spin-up procedure used for CTEM-GEM and the change in meteorological forcing, the simulation driven by retrieved fluxes (CT2013B) is similar to that achieved with CLASS-CTEM prior fluxes. This result is consistent with the finding of (Ott et al., 2015) that large differences in prior flux estimates result in only small differences in CO_2 concentrations. The reason is that once the fluxes enter the atmosphere, the gradients they create are slowly smoothed out by various modes of atmospheric variability. Thus, concentrations reflect the time integrated history of past fluxes smoothed by atmospheric mixing.

4.3 Inversion Analyses

The results in the previous two sections revealed that the GEM-MACH-GHG simulation of atmospheric CO_2 using CTEM-GEM and CTEM-CRUNCEP fluxes are comparable. They also indicate that the model driven with CTEM-GEM fluxes is able to reproduce temporal variations in atmospheric CO_2 at the selected sites. Since CTEM-GEM will be used as the land component of EC-CAS, which is presently under development and thus not yet available, here we use the GEOS-Chem data assimilation system to examine the impact on regional flux estimates of using CTEM-GEM and CTEM-CRUNCEP as prior fluxes in the context of an atmospheric CO_2 inversion analysis. To determine how the retrieved fluxes obtained with the two

Geosci. Model Dev. Discuss., https://doi.org/10.5194/gmd-2017-169
Manuscript under review for journal Geosci. Model Dev.
Discussion started: 11 September 2017

CTEM-based priors compare to other documented inverse modelling results, we also perform an inversion analysis using BEPS prior fluxes, which is the ecosystem model used in the GEOS-Chem inversions of Deng et al. (2014, 2016), and we compare our results to the retrieved fluxes from CT2013.

4.3.1 Seasonal Cycle of the Flux Estimates

Figure 12 shows the seasonal cycle of the a posteriori NEE from the GEOS-Chem inversion analyses using the three different a priori estimates of NEE (CTEM-GEM, CTEM-CRUNCEP, and BEPS), together with the optimized NEE from CT2013B. The a priori NEE from CTEM-GEM, CTEM-CRUNCEP and BEPS are also shown. For northern land, there is good agreement between the optimized NEE in terms of the amplitude and the growing season, except in boreal Eurasia where the peak carbon uptake is greatest for CT2013B. Since the range of various posteriors can be taken as an estimate of the uncertainty of flux retrievals (e.g., Gurney et al., 2004; Peylin et al., 2013), we conclude that the CTEM-based posterior estimates for most northern land regions are comparable to those from CT2013B and BEPS. This occurs because the surface observation network can reasonably constrain the northern extratropical latitudes (Peylin et al., 2013). However, the spread between the fluxes is larger in the tropical regions, where NEE seasonal cycles show less agreement in both phase and magnitude. There are large differences in the seasonal cycle between the CTEM-based fluxes (CTEM-CRUNCEP and CTEM-GEM) and the BEPS-based fluxes in northern Africa and tropical South America that are present in both the prior and posterior fluxes. As a result of the limited observational coverage in the tropics, the posterior fluxes are strongly influenced by the prior fluxes. Consequently, the differences in the prior fluxes across the inversions are reflected in the posterior fluxes. Similarly, in the southern extratropics the posterior fluxes primarily reflect the prior flux distributions due to the sparsity of observations. This result is consistent with that of Peylin et al. (2013) who also found more disagreement of various inversion results in the tropics and southern hemisphere.

The amplitude of seasonal cycle of the optimized NEE from CTEM-CRUNCEP is significantly reduced compared to the a priori seasonal cycle in almost all land regions. The changes in the amplitude of the seasonal cycle for CTEM-GEM are smaller than those for CTEM-CRUNCEP. This might indicate that CTEM-GEM has the ability to simulate the seasonal cycle of CO_2 fluxes that is more consistent with the atmospheric CO_2 signal.

4.3.2 Annual Mean Flux Estimates

The total annual a priori and a posteriori NEE from the GEOS-Chem inversion analyses for 2009-2010 are shown in Fig. 13 for the 11 land TransCom regions, along with the optimized values from CT2013B. Note that the tropical Asia panel has a different scale. All models estimate a sink (both for the a priori and the a posteriori) for the North America temperate, South American tropical, and Eurasian regions (except for temperate Eurasia, which has a source for CTEM-GEM prior). The largest difference between the a priori and a posteriori NEE in terms of the sign and magnitude were obtained for the Southern American temperate and Northern and Southern African regions. This is due to the fact that the tropics and Southern Hemisphere are poorly constrained by the current CO_2 network. Although the CT2013B fluxes tend to have stronger uptake in boreal Eurasia and the two African regions, BEPS has the largest uptake in the extra-tropical regions (North America temperate,

Geosci. Model Dev. Discuss., https://doi.org/10.5194/gmd-2017-169
Manuscript under review for journal Geosci. Model Dev.
Discussion started: 11 September 2017

Europe, Eurasia temperate) and tropical Asia. Some of the difference between CT2013B and all of the GEOS-Chem estimates can be attributed to different transport models and configurations of data assimilation (Peylin et al., 2013) used in GEOS-Chem and CT2013B (uses Tracer Transport Model - version 5 (TM5) (Peters et al., 2007)). Figure 13 also indicates that, for 2009, GEOS-Chem allocates the strongest sink in Tropical Asia for CTEM-CRUNCEP (2 Pg C year^{-1}). Given that the inversion with CTEM-CRUNCEP fluxes suggest much weaker sinks (or larger sources) for the South American Tropical and Northern African regions compared to CTEM-GEM and BEPS, we suspect that stronger uptake in tropical Asia could reflect the inversion compensating for the larger sources in tropical south America and northern Africa. The hypothesis is that CTEM-CRUNCEP start with a larger a priori sink in tropical Asia and it gets enhanced in the inversion to compensate for the other tropical regional biases.

Figure 14 shows the global annual totals of NEE (a priori and a posteriori) for 2009-2010, as well as annual totals, aggregated into three latitudinal bands: Southern Hemisphere (SH):90 S - 30° S, Tropics (TR): 30° S - 30° N, and Northern Hemisphere (NH): 30° N - 90° N). At the global scale, there is a good agreement between the optimized NEE in terms of magnitude. This indicates that the observations sufficiently constrain the global carbon budget so that the choice of prior fluxes is not critical. This is in agreement with Bruhwiler et al. (2011) who examine the impact of changing observation networks on flux estimates. However, optimized NEE for the three latitudinal bands show some differences, mainly in the tropics, where the observational coverage is poor.

These results are consistent with previous findings (e.g., Peters et al., 2007; Miller et al., 2015), which showed that optimized CO_2 fluxes in inversion analyses are heavily influenced by the spatial patterns in the a priori CO_2 fluxes, particularly in regions where observations are sparse (i.e. tropics and southern Hemisphere).

4.3.3 Evaluation of the Inversions

To more effectively evaluate the assimilation results, we compare the a posteriori CO_2 fields with independent data that were not ingested in the assimilation. Listed in Table 4 are the mean differences and root-mean-square errors (RMSEs) of the a posteriori CO_2 relative to TCCON data in 2009 and 2010. All three fluxes reproduce the TCCON data well, but the BEPS-based CO_2 fields have the smallest RMSEs of 1.22 ppm and 1.18 ppm with respect to the data in 2009 and 2010, respectively. We find that the RMSEs for the CO_2 fields based on the CTEM-GEM fluxes are smaller than those from the CTEM-CRUNCEP fluxes, with values of 1.24 ppm and 1.39 ppm in 2009 and 2010, compared to 1.42 ppm in both years for the fields from CTEM-CRUNCEP fluxes. We also compare the a posteriori CO_2 fields with HIPPO aircraft data in the lower troposphere (see Table 5). As with the comparison to TCCON data, we find that the a posteriori fields based on BEPS fluxes produce the smallest RMSEs relative to the aircraft data, with the fields from CTEM-GEM fluxes producing smaller RMSEs than those obtained from the CTEM-CRUNCEP fluxes. For the HIPPO-1 campaign, the a posteriori fields based on CTEM-CRUNCEP fluxes produce the smallest mean difference (-0.01 ppm), whereas for HIPPO-2 and HIPPO-3 the a posteriori CO_2 fields based on the BEPS and CTEM-GEM fluxes produce the smallest mean differences (-0.41 ppm and 0.16 ppm), respectively. Overall, the comparisons show that that CTEM-GEM provides relatively better agreement (in terms of the RMSEs) with the independent observations

Geosci. Model Dev. Discuss., https://doi.org/10.5194/gmd-2017-169
Manuscript under review for journal Geosci. Model Dev.
Discussion started: 11 September 2017

compared to CTEM-CRUNCEP. This implies that the spatial pattern of the a priori fluxes from CTEM-GEM provides a better constraint than CTEM-CRUNCEP for the inversion system.

5 Conclusions

CLASS-CTEM will be used to provide first-guess (a priori) terrestrial fluxes for the Environment Canada Carbon Assimilation System (EC-CAS) (Polavarapu et al., 2016). The transport model of EC-CAS that relates surface fluxes to atmospheric CO_2 concentrations is based on the GEM-MACH-GHG model (Polavarapu et al., 2016). To ensure consistency between the land and transport model, CLASS-CTEM will be driven by the standard meteorological forcing simulated (24 h forecast) by GEM-MACH-GHG. Therefore, the main focus of this study was to assess the impact of using the meteorological inputs from GEM-MACH-GHG in simulating both regional and global carbon fluxes by CLASS-CTEM.

We first evaluated the quality of the meteorological inputs from GEM-MACH-GHG against the standard meteorological forcing (CRU-NCEP) that is used to drive the latest versions of CLASS-CTEM, as well as against observation-based or reanalysis datasets. The comparison between the datasets indicates that the meteorological fields from GEM-MACH-GHG used in this study are similar in quality to those from observations-based datasets (CRU and CRU-NCEP) and reanalysis (ERA-Interim). The comparison also shows that radiation and temperature data from GEM-MACH-GHG and CRU-NCEP are in good agreement. However, there are some notable discrepancies between GEM and CRU-NCEP in terms of seasonal variations and spatial patterns of precipitation estimates, especially in the tropics, with GEM being drier than CRU-NCEP, ERA-Interim, and CRU. That might indicate that the convective scheme used in GEM-MACH-GHG system needs to be improved in particular over the tropics.

The differences in the precipitation fields between GEM-MACH-GHG and CRU-NCEP was reflected in the estimated carbon fluxes (GPP and R_{eco}). The amplitude and, to a lesser extent, the phase of the seasonal cycle are different between the two simulations, especially in the tropics. This is consistent with the findings of Dalmonech et al. (2015), who found that meteorological biases significantly control the magnitude of the productivity rather than the phenology and the seasonal cycle of carbon fluxes. Fluxes produced with GEM meteorology were obtained using a modified spin-up procedure based on current climate only. While it is clearly unsatisfactory to use a short climatology to spin-up carbon pools, it is an inevitable problem when coupling a TEM to an assimilation system since the latter focus on only a few years at a time. Moreover, operational weather assimilation systems are constantly changing so long datasets of analyses are simply not possible to obtain. Despite the deficiencies in the spin-up procedure, the fluxes produced from CTEM-GEM were comparable in quality to those produced from CTEM-CRUNCEP. Moreover, the global constraint from observations is sufficient to determine the global budget irrespective of the choice of a priori flux. In fact, some inverse models use a neutral annual a priori flux to better assess the ability of the observations to constrain the flux estimates (Deng et al., 2014). However, regional flux estimates are affected by the choice of a priori flux, particularly in data poor regions such as the tropics and southern hemisphere. Overall, the CTEM-GEM prior flux estimates are within the range of the other estimates from BEPS or top-down approaches (i.e. CT2013B), despite the significant differences in the model structure/approaches. However, flux estimates over the tropics from CTEM-GEM should

Geosci. Model Dev. Discuss., https://doi.org/10.5194/gmd-2017-169
Manuscript under review for journal Geosci. Model Dev.
Discussion started: 11 September 2017

be treated with caution due to the negative biases in the precipitation fields compared to all other datasets (i.e. ERA-Interim, CRU, and CRU-NCEP).

To assess their ability to model CO_2 at monitoring stations, NEE fluxes from CTEM-CRUNCEP and CTEM-GEM were used as a priori land fluxes in the GEM-MACH-GHG global atmospheric CO_2 transport model. The comparison indicated that the simulated CO_2 based on CTEM-GEM compared reasonably well with observed CO_2 in terms of temporal variations. However, the time series of the modelled CO_2 at the two selected sites indicated some difficulties in capturing the seasonal cycle of the observations, which can be attributed to the deficiencies in simulating the seasonal cycle of NEE from CLASS-CTEM in terms of phase as well as the magnitude, especially for the fluxes based on the CRU-NCEP meteorological data. The deficiencies in simulating the seasonal cycle was also noticed in the study by Arora et al. (2009), who compared simulated monthly CO_2 from CanESM1 (CTEM used as the land component of that model) against observations at selected sites and found that there was a shift in the seasonal cycle (about a month later) at Barrow, Niwot Ridge, and Mauna Loa (see their Figure 11). The study by Anav et al. (2013), which compared 18 Earth system models, also showed that CanESM2 has some limitations reproducing the net uptake of carbon during spring and summer months.

To examine the impact of using fluxes from CTEM-GEM and CTEM-CRUNCEP as a priori flux estimates in atmospheric inversion analyses, we used the GEOS-Chem data assimilation system since EC-CAS is still under development. We assimilated in situ atmospheric CO_2 observations from the surface network to estimate optimized monthly mean NEE fluxes for 2009-2010. The time series of the estimated fluxes, integrated over different land regions, revealed that the optimized NEE is shifted from its a priori pattern in order to fit the data. For comparison with the CTEM-based fluxes we also used BEP fluxes (Deng et al., 2014) as an a priori in the inversion analyses. We found that the CTEM-based optimized fluxes produced atmospheric CO_2 concentrations that were consistent with those based on BEPS. For example, the mean differences between independent TCCON data in 2010 and the modeled CO_2 based the CTEM-GEM, CTEM-CRUNCEP, and BEPS optimized fluxes were 0.80, 0. 78, and 0.54 ppm, with RMSEs of 1.39, 1.42, and 1.18 ppm, respectively. For observations from the HIPPO-3 aircraft campaign, the mean differences between the observations and the CO_2 simulated from the optimized CTEM-GEM, CTEM-CRUNCEP, and BEPS fluxes were 0.16, 0.26, -0.28 ppm, with RMSEs of 0.94, 1.04, and 0.87 ppm, respectively. The results are promising for the EC-CAS project as they demonstrate that the CTEM-GEM fluxes can provide useful a priori fluxes for the global inversion system. When incorporated into the GEOS-Chem assimilation system, the inversion is capable of correcting the CTEM-GEM fluxes over annual and seasonal time scales in order to match the variability in the atmospheric data. In addition, the results of the optimized fluxes as well as the comparison of the a posteriori CO_2 to observations suggests that the spatial pattern of the a priori fluxes from CTEM-GEM provide a better constraint than CTEM-CRUNCEP for the inversion system.

Finally, this study provided insights into the deficiencies in the model, and data constraints (both meteorological and atmospheric CO_2 data). By coupling CLASS-CTEM into EC-CAS, a CCDAS approach becomes possible where observational constraints give feedback on a TEM. Ultimately, such an approach can help to improve the performance of CLASS-CTEM, and thus improve the CanESM which is used to address the question of the feedback between climate change and the carbon cycle.

Code and data availability. Fortran code for CLASS-CTEM modelling frame-work is available on request and upon agreeing to ECCC's licensing agreement available at: http://collaboration.cmc.ec.gc.ca/science/rpn.comm. Please contact the coauthor, Joe Melton (joe.melton@canada.ca), to obtain model code. The GEM and GEM-MACH source codes are integrated into the unique operational computing environments of ECCC. These source codes are copyrighted but are available upon request subject to the GNU Lesser General Public License (LGPL v2.1) agreement (contact the coauthor, Michael Neish (Michael.Neish@canada.ca)). Some documentation on GEM is available at: http://collaboration.cmc.ec.gc.ca/science/rpn/gem/gemdm/gemdm.html and http://collaboration.cmc.ec.gc.ca/science/rpn/gef_html_public/. ECCCs model output data are available at: https://weather.gc.ca/grib/index_e.html. The GEOS-Chem model, including the adjoint code, is freely available to the public and is distributed through GitLab. Instructions for obtaining and running the model are available on the GEOS-Chem wiki: (http://wiki.seas.harvard.edu/geos-chem/). The NOAA in situ CO2 observations used in the inversion analysis are available from ftp://aftp.cmdl.noaa.gov/data/trace_gases/co2/flask/surface/. All data generated by CLASS-CTEM is available from ECCC upon completion of a licensing agreement.

Author contributions. Bakr Badawy and Saroja Polavarapu designed the experiments. Bakr Badawy generated the required meteorological fields for CLASS-CTEM from GEM-MACH-GHG and performed the simulations for CLASS-CTEM and GEM-MACH-GHG and analysed the experiments and created the figures. Feng Deng performed the simulations for GEOS-Chem in coordination with Dylan Jones who contributed to the analysis and the interpretation of the assimilation results. Michael Neish developed and contributed to the GEM-MACH-GHG model diagnostics. Joe Melton and Vivek Arora provided the code of CLASS-CTEM used in this study and provided input on the implementation of the model. Ray Nassar provided helpful discussions. Bakr Badawy prepared the manuscript with contributions from all co-authors.

Competing interests. The authors declare that they have no conflict of interest.

Acknowledgements. Bakr Badawy was supported by Environment and Climate Change Canada (ECCC). We gratefully acknowledge all the data providers including the NOAA CarbonTracker assimilation system team for making their model products publicly available at http://carbontracker.noaa.gov. The NOAA in situ CO_2 observations used in the inversion analysis are available from https://www.esrl.noaa.gov/gmd/dv/data/. We also would like to thank Doug Worthy for developing and maintaining ECCCs greenhouse gas measurement network and for providing the CO_2 concentration measurements. We gratefully acknowledge TCCON PIs (cited in Table 1) for making their data available. TCCON data were obtained from the TCCON Data Archive, hosted by the Carbon Dioxide Information Analysis Center (CDIAC) - tccon.onrl.gov. We gratefully thank the HIPPO (HIAPER Pole-to-Pole Observations, National ScienceFoundation, NSF, NSF/NCAR Gulfstream-V (GV)) science team for making their data freely available at http://hippo.ornl.gov. The collection of the original HIPPO data were supported by NSF and NOAA. ERA-Interim data used in this study have been obtained from the ECMWF data server: http://data.ecmwf.int/data. We thank Douglas Chan who evaluated the manuscript for the internal review process at ECCC and provided helpful comments, which improved the manuscript.

Geosci. Model Dev. Discuss., https://doi.org/10.5194/gmd-2017-169
Manuscript under review for journal Geosci. Model Dev.
Discussion started: 11 September 2017

Geoscientific Model Development Discussions
Open Access
EGU

References

Agusti-Panareda, A., Massart, S., Chevallier, F., Boussetta, S., Balsamo, G., Beljaars, A., Ciais, P., Deutscher, N. M., Engelen, R., Jones, L., Kivi, R., Paris, J.-D., Peuch, V.-H., Sherlock, V., Vermeulen, A. T., Wennberg, P. O., and Wunch, D.: Forecasting global atmospheric CO_2, Atmospheric Chemistry and Physics, 14, 11 959–11 983, https://doi.org/10.5194/acp-14-11959-2014, http://www.atmos-chem-phys.net/14/11959/2014/, 2014.

Agusti-Panareda, A., Diamantakis, M., Bayona, V., Klappenbach, F., and Butz, A.: Improving the inter-hemispheric gradient of total column atmospheric CO_2 and CH_4 in simulations with the ECMWF semi-Lagrangian atmospheric global model, Geoscientific Model Development Discussions, 2016, 1–31, https://doi.org/10.5194/gmd-2016-143, http://www.geosci-model-dev-discuss.net/gmd-2016-143/, 2016.

Anav, A., Friedlingstein, P., Kidston, M., Bopp, L., Ciais, P., Cox, P., Jones, C., Jung, M., Myneni, R., and Zhu, Z.: Evaluating the Land and Ocean Components of the Global Carbon Cycle in the CMIP5 Earth System Models, Journal of Climate, 26, 6801–6843, https://doi.org/10.1175/JCLI-D-12-00417.1, http://dx.doi.org/10.1175/JCLI-D-12-00417.1, 2013.

Anav, A., Friedlingstein, P., Beer, C., Ciais, P., Harper, A., Jones, C., Murray-Tortarolo, G., Papale, D., Parazoo, N. C., Peylin, P., Piao, S., Sitch, S., Viovy, N., Wiltshire, A., and Zhao, M.: Spatiotemporal patterns of terrestrial gross primary production: A review, Reviews of Geophysics, 53, 785–818, https://doi.org/10.1002/2015RG000483, http://dx.doi.org/10.1002/2015RG000483, 2015RG000483, 2015.

Arora, V. K.: Simulating energy and carbon fluxes over winter wheat using coupled land surface and terrestrial ecosystem models, Agricultural and Forest Meteorology, 118, 21–47, 2003.

Arora, V. K. and Boer, G. J.: Fire as an interactive component of dynamic vegetation models, Journal of Geophysical Research-Biogeosciences, 110, G02 008, doi:10.1029/2005JG000 042, 2005.

Arora, V. K. and Boer, G. J.: Uncertainties in the 20th century carbon budget associated with land use change, Global Change Biology, 16, 3327–3348, https://doi.org/10.1111/j.1365-2486.2010.02202.x, 2010.

Arora, V. K., Boer, G. J., Christian, J. R., Curry, C. L., Denman, K. L., Zahariev, K., Flato, G. M., Scinocca, J. F., Merryfield, W. J., and Lee, W. G.: The Effect of Terrestrial Photosynthesis Down Regulation on the Twentieth-Century Carbon Budget Simulated with the CCCma Earth System Model, J. Climate, 22, 6066–6088, https://doi.org/10.1175/2009JCLI3037.1, 2009.

Arora, V. K., Boer, G. J., Friedlingstein, P., Eby, M., Jones, C. D., Christian, J. R., Bonan, G., Bopp, L., Brovkin, V., Cadule, P., Hajima, T., Ilyina, T., Lindsay, K., Tjiputra, J. F., and Wu, T.: Carbon-Concentration and Carbon-Climate Feedbacks in CMIP5 Earth System Models, Journal of Climate, 26, 5289–5314, https://doi.org/10.1175/JCLI-D-12-00494.1, http://dx.doi.org/10.1175/JCLI-D-12-00494.1, 2013.

Badawy, B., Rödenbeck, C., Reichstein, M., Carvalhais, N., and Heimann, M.: Technical Note: The Simple Diagnostic Photosynthesis and Respiration Model (SDPRM), Biogeosciences, 10, 6485–6508, https://doi.org/10.5194/bg-10-6485-2013, 2013.

Badawy, B., Arora, V. K., Melton, J. R., and Nassar, R.: Modeling the diurnal variability of respiratory fluxes in the Canadian Terrestrial Ecosystem Model (CTEM), J. Adv. Model. Earth Syst., 8, 614–633, http://dx.doi.org/10.1002/2015MS000540, 2016.

Balsamo, G., Boussetta, S., Lopez, P., and Ferranti, L.: Evaluation of ERA-Interim and ERA-Interim GPCP-rescaled precipitation over the U.S.A., ERA Report Series 5, pp. 10., ECMWF, Reading, England, 2010.

Beer, C., Reichstein, M., Tomelleri, E., Ciais, P., Jung, M., Carvalhais, N., Roedenbeck, C., and et. al.: Terrestrial Gross Carbon Dioxide Uptake: Global Distribution and Covariation with Climate, Science, 329, 834, 2010.

Berrisford, P., Dee, D., Poli, P., Brugge, R., Fielding, K., Fuentes, M., Kållberg, P., Kobayashi, S., Uppala, S., and Simmons, A.: The ERA-Interim archive Version 2.0, Shinfield Park, Reading, 2011.

Blumenstock, T., Hase, F., Schneider, M., Garcia, O., and Sepulveda, E.: TCCON data from Izana, Tenerife, Spain, Release GGG2014R0, http://dx.doi.org/10.14291/tccon.ggg2014.izana01.R0/1149295, https://doi.org/10.14291/tccon.ggg2014.izana01.R0/1149295, TCCON data archive, hosted by the Carbon Dioxide Information Analysis Center, Oak Ridge National Laboratory, Oak Ridge, Tennessee, U.S.A., 2014.

Bruhwiler, L. M. P., Michalak, A. M., and Tans, P. P.: Spatial and temporal resolution of carbon flux estimates for 1983-2002, Biogeosciences, 8, 1309–1331, https://doi.org/10.5194/bg-8-1309-2011, http://www.biogeosciences.net/8/1309/2011/, 2011.

Carvalhais, N., Reichstein, M., Seixas, J., Collatz, G. J., Pereira, J. S., Berbigier, P., Carrara, A., Granier, A., Montagnani, L., Papale, D., Rambal, S., Sanz, M. J., and Valentini, R.: Implications of the carbon cycle steady state assumption for biogeochemical modeling performance and inverse parameter retrieval, Global Biogeochemical Cycles, 22, https://doi.org/10.1029/2007GB003033, http://dx.doi.org/10.1029/2007GB003033, gB2007, 2008.

Carvalhais, n., reichstein, m., ciais, p., collatz, g. j., mahecha, m. d., montagnani, l., papale, d., rambal, s., and seixas, j.: Identification of vegetation and soil carbon pools out of equilibrium in a process model via eddy covariance and biometric constraints, Global Change Biology, 16, 2813–2829, https://doi.org/10.1111/j.1365-2486.2010.02173.x, http://dx.doi.org/10.1111/j.1365-2486.2010.02173.x, 2010.

Charron, M., Polavarapu, S., Buehner, M., Vaillancourt, P. A., Charette, C., Roch, M., Morneau, J., Garand, L., Aparicio, J. M., MacPherson, S., Pellerin, S., St-James, J., and Heilliette, S.: The Stratospheric Extension of the Canadian Global Deterministic Medium-Range Weather Forecasting System and Its Impact on Tropospheric Forecasts, Monthly Weather Review, 140, 1924–1944, https://doi.org/10.1175/MWR-D-11-00097.1, http://dx.doi.org/10.1175/MWR-D-11-00097.1, 2012.

Chen, J. M., Mo, G., Pisek, J., Liu, J., Deng, F., Ishizawa, M., and Chan, D.: Effects of foliage clumping on the estimation of global terrestrial gross primary productivity, Global Biogeochemical Cycles, 26, https://doi.org/10.1029/2010GB003996, http://dx.doi.org/10.1029/2010GB003996, gB1019, 2012.

Clein, J., McGuire, A. D., Euskirchen, E. S., and Calef, M.: The Effects of Different Climate Input Datasets on Simulated Carbon Dynamics in the Western Arctic, Earth Interactions, 11, 1–24, https://doi.org/10.1175/EI229.1, http://dx.doi.org/10.1175/EI229.1, 2007.

Côté, J., Gravel, S., Méthot, A., Patoine, A., Roch, M., and Staniforth, A.: The Operational CMC-MRB Global Environmental Multi-scale (GEM) Model. Part I: Design Considerations and Formulation, Mon. Wea. Rev., 126, 1373–1395, https://doi.org/10.1175/1520-0493(1998)126<1373:TOCMGE>2.0.CO;2, http://dx.doi.org/10.1175/1520-0493(1998)126<1373:TOCMGE>2.0.CO;2, 1998a.

Dalmonech, D., Zaehle, S., Schuermann, G. J., Brovkin, V., Reick, C., and Schnur, R.: Separation of the Effects of Land and Climate Model Errors on Simulated Contemporary Land Carbon Cycle Trends in the MPI Earth System Model version 1, Journal of Climate, 28, 272–291, https://doi.org/10.1175/JCLI-D-13-00593.1, http://dx.doi.org/10.1175/JCLI-D-13-00593.1, 2015.

Dee, D. P., Uppala, S. M., Simmons, A. J., Berrisford, P., Poli, P., Kobayashi, S., Andrae, U., Balmaseda, M. A., Balsamo, G., Bauer, P., Bechtold, P., Beljaars, A. C. M., van de Berg, L., Bidlot, J., Bormann, N., Delsol, C., Dragani, R., Fuentes, M., Geer, A. J., Haimberger, L., Healy, S. B., Hersbach, H., Hólm, E. V., Isaksen, L., Kallberg, P., Köhler, M., Matricardi, M., McNally, A. P., Monge-Sanz, B. M., Morcrette, J.-J., Park, B.-K., Peubey, C., de Rosnay, P., Tavolato, C., Thépaut, J.-N., and Vitart, F.: The ERA-Interim reanalysis: configuration and performance of the data assimilation system, Quarterly Journal of the Royal Meteorological Society, 137, 553–597, https://doi.org/10.1002/qj.828, http://dx.doi.org/10.1002/qj.828, 2011.

Deng, F. and Chen, J. M.: Recent global CO_2 flux inferred from atmospheric CO_2 observations and its regional analyses, Biogeosciences, 8, 3263–3281, https://doi.org/10.5194/bg-8-3263-2011, http://www.biogeosciences.net/8/3263/2011/, 2011.

Deng, F., Jones, D. B. A., Henze, D. K., Bousserez, N., Bowman, K. W., Fisher, J. B., Nassar, R., O'Dell, C., Wunch, D., Wennberg, P. O., Kort, E. A., Wofsy, S. C., Blumenstock, T., Deutscher, N. M., Griffith, D. W. T., Hase, F., Heikkinen, P., Sherlock, V., Strong, K., Sussmann,

R., and Warneke, T.: Inferring regional sources and sinks of atmospheric CO_2 from GOSAT XCO_2 data, Atmospheric Chemistry and Physics, 14, 3703–3727, https://doi.org/10.5194/acp-14-3703-2014, http://www.atmos-chem-phys.net/14/3703/2014/, 2014.

Deng, F., Jones, D. B. A., O'Dell, C. W., Nassar, R., and Parazoo, N. C.: Combining GOSAT X CO_2 observations over land and ocean to improve regional CO_2 flux estimates, Journal of Geophysical Research: Atmospheres, 121, 1896–1913, https://doi.org/10.1002/2015JD024157, http://dx.doi.org/10.1002/2015JD024157, 2015JD024157, 2016.

Deutscher, N., Notholt, J., Messerschmidt, J., Weinzierl, C., Warneke, T., Petri, C., Grupe, P., and Katrynski, K.: TCCON data from Bialystok, Poland, Release GGG2014R1, http://dx.doi.org/10.14291/tccon.ggg2014.bialystok01.R1/1183984, https://doi.org/10.14291/tccon.ggg2014.bialystok01.R1/1183984, TCCON data archive, hosted by the Carbon Dioxide Information Analysis Center, Oak Ridge National Laboratory, Oak Ridge, Tennessee, U.S.A., 2014.

Dlugokencky, E., Lang, P., Masarie, K., Crotwell, A., and Crotwell, M.: Atmospheric Carbon Dioxide Dry Air Mole Fractions from the NOAA ESRL Carbon Cycle Cooperative Global Air Sampling Network, 1968-2014, Version: 2015-08-03, ftp://aftp.cmdl.noaa.gov/data/trace_gases/co2/flask/surface/, 2015.

Exbrayat, J.-F., Pitman, A. J., and Abramowitz, G.: Response of microbial decomposition to spin-up explains CMIP5 soil carbon range until 2100, Geoscientific Model Development, 7, 2683–2692, https://doi.org/10.5194/gmd-7-2683-2014, http://www.geosci-model-dev.net/7/2683/2014/, 2014.

Friedlingstein, P., Cox, P., Betts, R., Bopp, L., von Bloh, W., Brovkin, V., Cadule, P., Doney, S., Eby, M., Fung, I., Bala, G., John, J., Jones, C., Joos, F., Kato, T., Kawamiya, M., Knorr, W., Lindsay, K., Matthews, H. D., Raddatz, T., Rayner, P., Reick, C., Roeckner, E., Schnitzler, K.-G., Schnur, R., Strassmann, K., Weaver, A. J., Yoshikawa, C., and Zeng, N.: Climate-Carbon Cycle Feedback Analysis: Results from the C4MIP Model Intercomparison, J. Climate, 19, 3337–3353, https://doi.org/10.1175/JCLI3800.1, 2006.

Friedlingstein, P., Meinshausen, M., Arora, V. K., Jones, C. D., Anav, A., Liddicoat, S. K., and Knutti, R.: Uncertainties in CMIP5 Climate Projections due to Carbon Cycle Feedbacks, Journal of Climate, 27, 511–526, https://doi.org/10.1175/JCLI-D-12-00579.1, http://dx.doi.org/10.1175/JCLI-D-12-00579.1, 2014.

Garnaud, C., Sushama, L., and Arora, V. K.: The effect of driving climate data on the simulated terrestrial carbon pools and fluxes over North America, International Journal of Climatology, 34, 1098–1110, https://doi.org/10.1002/joc.3748, 2014.

Girard, C., Plante, A.and Desgagné, M., McTaggart-Cowan, R., Côté, J., Charron, M., Gravel, S., Lee, V., Patoine, A., Qaddouri, A., Roch, M., Spacek, L., Tanguay, M., Vaillancourt, P. A., and Zadra, A.: Staggered Vertical Discretization of the Canadian Environmental Multiscale (GEM) Model Using a Coordinate of the Log-Hydrostatic-Pressure Type, Mon. Wea. Rev., 142, 1183–1196, https://doi.org/10.1175/MWR-D-13-00255.1, http://dx.doi.org/10.1175/MWR-D-13-00255.1, 2013.

Griffith, D. W. T., Deutscher, N., Velazco, V. A., Wennberg, P. O., Yavin, Y., Aleks, G. K., Washenfelder, R., Toon, G. C., Blavier, J.-F., Murphy, C., Jones, N., Kettlewell, G., Connor, B., Macatangay, R., Roehl, C., Ryczek, M., Glowacki, J., Culgan, T., and Bryant, G.: TCCON data from Darwin, Australia, Release GGG2014R0, http://dx.doi.org/10.14291/tccon.ggg2014.darwin01.R0/1149290, https://doi.org/10.14291/tccon.ggg2014.darwin01.R0/1149290, TCCON data archive, hosted by the Carbon Dioxide Information Analysis Center, Oak Ridge National Laboratory, Oak Ridge, Tennessee, U.S.A., 2014a.

Griffith, D. W. T., Velazco, V. A., Deutscher, N., Murphy, C., Jones, N., Wilson, S., Macatangay, R., Kettlewell, G., Buchholz, R. R., and Riggenbach, M.: TCCON data from Wollongong, Australia, Release GGG2014R0, http://dx.doi.org/10.14291/tccon.ggg2014.wollongong01.R0/1149291, https://doi.org/10.14291/tccon.ggg2014.wollongong01.R0/1149291, TCCON data archive, hosted by the Carbon Dioxide Information Analysis Center, Oak Ridge National Laboratory, Oak Ridge, Tennessee, U.S.A., 2014b.

Gurney, K. R., Law, R. M., Denning, A. S., Rayner, P. J., Baker, D., Bousquet, P., Bruhwiler, L., Chen, Y.-H., Ciais, P., Fan, S. M., Fung, I. Y., Gloor, M., Heimann, M., Higuchi, K., John, J., Kowalczyk, E., Maki, T., Maksyutov, S., Peylin, P., Prather, M., Pak, B. C., Sarmiento, J., Taguchi, S., Takahashi, T., and Yuen, C.-W.: TransCom 3 CO_2 inversion intercomparison: 1. Annual mean control results and sensitivity to transport and prior flux information, Tellus Series B-Chemical and Physical Meteorology, 55, 555–579, 2003.

Gurney, K. R., Law, R. M., Denning, A. S., Rayner, P. J., Pak, B. C., Baker, D., Bousquet, P., Bruhwiler, L., Chen, Y.-H., Ciais, P., Fung, I. Y., Heimann, M., John, J., Maki, T., Maksyutov, S., Peylin, P., Prather, M., and Taguchi, S.: Transcom 3 inversion intercomparison: Model mean results for the estimation of seasonal carbon sources and sinks, Global Biogeochemical Cycles, 18, GB1010, doi:10.1029/2003GB002 111, 2004.

Harris, I., Jones, P., Osborn, T., and Lister, D.: Updated high-resolution grids of monthly climatic observations - the CRU TS3.10 Dataset, Int. J. Climatol., 34, 623–642, http://dx.doi.org/10.1002/joc.3711, 2014.

Hase, F., Blumenstock, T., Dohe, S., Gross, J., and Kiel, M.: TCCON data from Karlsruhe, Germany, Release GGG2014R1, http://dx.doi.org/10.14291/tccon.ggg2014.karlsruhe01.R1/1182416, https://doi.org/10.14291/tccon.ggg2014.karlsruhe01.R1/1182416, TCCON data archive, hosted by the Carbon Dioxide Information Analysis Center, Oak Ridge National Laboratory, Oak Ridge, Tennessee, U.S.A., 2014.

Henze, D. K., Hakami, A., and Seinfeld, J. H.: Development of the adjoint of GEOS-Chem, Atmospheric Chemistry and Physics, 7, 2413–2433, https://doi.org/10.5194/acp-7-2413-2007, http://www.atmos-chem-phys.net/7/2413/2007/, 2007.

Houghton, R. A., House, J. I., Pongratz, J., van der Werf, G. R., DeFries, R. S., Hansen, M. C., Le Quéré, C., and Ramankutty, N.: Carbon emissions from land use and land-cover change, Biogeosciences, 9, 5125–5142, https://doi.org/10.5194/bg-9-5125-2012, http://www.biogeosciences.net/9/5125/2012/, 2012.

Huntzinger, D., Post, W., Wei, Y., Michalak, A., West, T., Jacobson, A., Baker, I., Chen, J., Davis, K., Hayes, D., Hoffman, F., Jain, A., Liu, S., McGuire, A., Neilson, R., Potter, C., Poulter, B., Price, D., Raczka, B., Tian, H., Thornton, P., Tomelleri, E., Viovy, N., Xiao, J., Yuan, W., Zeng, N., Zhao, M., and Cook, R.: North American Carbon Program (NACP) regional interim synthesis: Terrestrial biospheric model intercomparison , Ecological Modelling, 232, 144 – 157, https://doi.org/http://dx.doi.org/10.1016/j.ecolmodel.2012.02.004, http://www.sciencedirect.com/science/article/pii/S0304380012000725, 2012.

Huntzinger, D. N., Schwalm, C., Michalak, A. M., Schaefer, K., King, A. W., Wei, Y., Jacobson, A., Liu, S., Cook, R. B., Post, W. M., Berthier, G., Hayes, D., Huang, M., Ito, A., Lei, H., Lu, C., Mao, J., Peng, C. H., Peng, S., Poulter, B., Riccuito, D., Shi, X., Tian, H., Wang, W., Zeng, N., Zhao, F., and Zhu, Q.: The North American Carbon Program Multi-Scale Synthesis and Terrestrial Model Intercomparison Project - Part 1: Overview and experimental design, Geoscientific Model Development, 6, 2121–2133, https://doi.org/10.5194/gmd-6-2121-2013, http://www.geosci-model-dev.net/6/2121/2013/, 2013.

Hurtt, G., Chini, L., Frolking, S., Betts, R., Feddema, J., Fischer, G., Fisk, J., Hibbard, K., Houghton, R., Janetos, A., Jones, C., Kindermann, G., Kinoshita, T., Klein Goldewijk, K., Riahi, K., Shevliakova, E., Smith, S., Stehfest, E., Thomson, A., Thornton, P., van Vuuren, D., and Wang, Y.: Harmonization of land-use scenarios for the period 1500-2100: 600 years of global gridded annual land-use transitions, wood harvest, and resulting secondary lands, Climatic Change, 109, 117–161–, 2011.

Jung, M., Vetter, M., Herold, M., Churkina, G., Reichstein, M., Zaehle, S., Ciais, P., Viovy, N., Bondeau, A., Chen, Y., Trusilova, K., Feser, F., and Heimann, M.: Uncertainties of modeling gross primary productivity over Europe: A systematic study on the effects of using different drivers and terrestrial biosphere models, Global Biogeochemical Cycles, 21, https://doi.org/10.1029/2006GB002915, http://dx.doi.org/10.1029/2006GB002915, gB4021, 2007.

Jung, M., Reichstein, M., and Bondeau, A.: Towards global empirical upscaling of FLUXNET eddy covariance observations: validation of a model tree ensemble approach using a biosphere model, Biogeosciences, 6, 2013, 2009.

Kalnay, E., Kanamitsu, M., Kistler, R., Collins, W., Deaven, D., Gandin, L., Iredell, M., Saha, S., White, G., Woollen, J., Zhu, Y., Chelliah, M., Ebisuzaki, W., Higgins, W., Janowiak, J., Mo, K. C., Ropelewski, C., Wang, J., Leetmaa, A., Reynolds, R., Jenne, R., and Joseph, D.: The NCEP/NCAR 40-year reanalysis project, Bull. Am. Met. Soc., 77, 437–471, 1996.

Kaminski, T., Knorr, W., Schürmann, G., Scholze, M., Rayner, P. J., Zaehle, S., Blessing, S., Dorigo, W., Gayler, V., Giering, R., Gobron, N., Grant, J. P., Heimann, M., Hooker-Stroud, A., Houweling, S., Kato, T., Kattge, J., Kelley, D., Kemp, S., Koffi, E. N., Köstler, C., Mathieu, P.-P., Pinty, B., Reick, C. H., Rödenbeck, C., Schnur, R., Scipal, K., Sebald, C., Stacke, T., van Scheltinga, A. T., Vossbeck, M., Widmann, H., and Ziehn, T.: The BETHY/JSBACH Carbon Cycle Data Assimilation System: experiences and challenges, Journal of Geophysical Research: Biogeosciences, 118, 1414–1426, https://doi.org/10.1002/jgrg.20118, 2013.

Kivi, R., Heikkinen, P., and Kyro, E.: TCCON data from Sodankyla, Finland, Release GGG2014R0, http://dx.doi.org/10.14291/tccon.ggg2014.sodankyla01.R0/1149280, https://doi.org/10.14291/tccon.ggg2014.sodankyla01.R0/1149280, TCCON data archive, hosted by the Carbon Dioxide Information Analysis Center, Oak Ridge National Laboratory, Oak Ridge, Tennessee, U.S.A., 2014.

Koffi, E. N., Rayner, P. J., Scholze, M., Chevallier, F., and Kaminski, T.: Quantifying the constraint of biospheric process parameters by CO_2 concentration and flux measurement networks through a carbon cycle data assimilation system, Atmospheric Chemistry and Physics, 13, 10 555–10 572, https://doi.org/10.5194/acp-13-10555-2013, 2013.

Krinner, G., Viovy, N., de Noblet-Ducoudré, N., Ogée, J., Polcher, J., Friedlingstein, P., Ciais, P., Sitch, S., and Prentice, I. C.: A dynamic global vegetation model for studies of the coupled atmosphere-biosphere system, Global Biogeochemical Cycles, 19, GB1015, doi:10.1029/2003GB002 199, 2005.

Kuze, A., Suto, H., Nakajima, M., and Hamazaki, T.: Initial Onboard Performance of TANSO-FTS on GOSAT, in: Advances in Imaging, p. FTuC2, Optical Society of America, https://doi.org/10.1364/FTS.2009.FTuC2, http://www.osapublishing.org/abstract.cfm?URI=FTS-2009-FTuC2, 2009.

Makar, P., Gong, W., Milbrandt, J., Hogrefe, C., Zhang, Y., Curci, G., Žabkar, R., Im, U., Balzarini, A., Baró, R., Bianconi, R., Cheung, P., Forkel, R., Gravel, S., Hirtl, M., Honzak, L., Hou, A., Jiménez-Guerrero, P., Langer, M., Moran, M., Pabla, B., Pérez, J., Pirovano, G., José, R. S., Tuccella, P., Werhahn, J., Zhang, J., and Galmarini, S.: Feedbacks between air pollution and weather, Part 1: Effects on weather, Atmospheric Environment, 115, 442 – 469, https://doi.org/http://dx.doi.org/10.1016/j.atmosenv.2014.12.003, http://www.sciencedirect.com/science/article/pii/S1352231014009510, 2015.

McGuire, A. D., Sitch, S., Clein, J. S., Dargaville, R., Esser, G., Foley, J., Heimann, M., Joos, F., Kaplan, J., Kicklighter, D. W., Meier, R. A., Melillo, J. M., Moore III, B., Prentice, I. C., Ramankutty, N., Reichenau, T., Schloss, A., Tian, H., Williams, L. J., and Wittenberg, U.: Carbon balance of the terrestrial biosphere in the twentieth century: Analyses of CO_2, climate and land use effects with four process-based ecosystem models, Global Biogeochemical Cycles, 15, 183–206, 2001.

Meinshausen, M., Smith, S., Calvin, K., Daniel, J., Kainuma, M., Lamarque, J.-F., Matsumoto, K., Montzka, S., Raper, S., Riahi, K., Thomson, A., Velders, G., and van Vuuren, D.: The RCP greenhouse gas concentrations and their extensions from 1765 to 2300, Climatic Change, 109, 213–241–, 2011.

Melton, J. R. and Arora, V. K.: Sub-grid scale representation of vegetation in global land surface schemes: implications for estimation of the terrestrial carbon sink, Biogeosciences, 11, 1021–1036, https://doi.org/10.5194/bg-11-1021-2014, 2014.

Melton, J. R. and Arora, V. K.: Competition between plant functional types in the Canadian Terrestrial Ecosystem Model (CTEM) v. 2.0, Geoscientific Model Development, 9, 323–361, https://doi.org/doi:10.5194/gmd-9-323-2016, 2016.

Melton, J. R., Shrestha, R. K., and Arora, V. K.: The influence of soils on heterotrophic respiration exerts a strong control on net ecosystem productivity in seasonally dry Amazonian forests, Biogeosciences, 12, 1151–1168, https://doi.org/10.5194/bg-12-1151-2015, 2015.

Miller, S. M., Hayek, M. N., Andrews, A. E., Fung, I., and Liu, J.: Biases in atmospheric CO₂ estimates from correlated meteorology modeling errors, Atmospheric Chemistry and Physics, 15, 2903–2914, https://doi.org/10.5194/acp-15-2903-2015, http://www.atmos-chem-phys.net/15/2903/2015/, 2015.

Moran, M., Meńard, S., Talbot, D., Huang, P., Makar, P., Gong, W., Landry, H., Gravel, S., Gong, S., Crevier, L., Kallaur, A., and Sassi, M.: Particulate-matter forecasting with GEM-MACH15, a new Canadian air-quality forecast model, in: Steyn, D.G. and Rao, S.T (Eds.)s), Air Pollution Modelling and Its Application XX, Springer, Dordrecht, 2010.

Nassar, R., Jones, D. B. A., Suntharalingam, P., Chen, J. M., Andres, R. J., Wecht, K. J., Yantosca, R. M., Kulawik, S. S., Bowman, K. W., Worden, J. R., Machida, T., and Matsueda, H.: Modeling global atmospheric CO₂ with improved emission inventories and CO₂ production from the oxidation of other carbon species, Geoscientific Model Development, 3, 689–716, https://doi.org/10.5194/gmd-3-689-2010, http://www.geosci-model-dev.net/3/689/2010/, 2010.

Nemani, R. R., Keeling, C. D., Hashimoto, H., Jolly, W. M., Piper, S. C., Tucker, C. J., Myneni, R. B., and Running, S. W.: Climate-driven increases in global terrestrial net primary production from 1982 to 1999, Science, 300, 1560–1563, 2003.

Notholt, J., Petri, C., Warneke, T., Deutscher, N., Buschmann, M., Weinzierl, C., Macatangay, R., and Grupe, P.: TCCON data from Bremen, Germany, Release GGG2014R0, http://dx.doi.org/10.14291/tccon.ggg2014.bremen01.R0/1149275, https://doi.org/10.14291/tccon.ggg2014.bremen01.R0/1149275, TCCON data archive, hosted by the Carbon Dioxide Information Analysis Center, Oak Ridge National Laboratory, Oak Ridge, Tennessee, U.S.A., 2014.

Ott, L. E., Pawson, S., Collatz, G. J., Gregg, W. W., Menemenlis, D., Brix, H., Rousseaux, C. S., Bowman, K. W., Liu, J., Eldering, A., Gunson, M. R., and Kawa, S. R.: Assessing the magnitude of CO2 flux uncertainty in atmospheric CO2 records using products from NASA's Carbon Monitoring Flux Pilot Project, Journal of Geophysical Research: Atmospheres, 120, 734–765, https://doi.org/10.1002/2014JD022411, http://dx.doi.org/10.1002/2014JD022411, 2014JD022411, 2015.

Peters, W., Jacobson, A. R., Sweeney, C., Andrews, A. E., Conway, T. J., Masarie, K., Miller, J. B., Bruhwiler, L. M. P., Pétron, G., Hirsch, A. I., Worthy, D. E. J., van der Werf, G. R., Randerson, J. T., Wennberg, P. O., Krol, M. C., and Tans, P. P.: An atmospheric perspective on North American carbon dioxide exchange: CarbonTracker, PNAS, 104, 18 925–18 930, 2007.

Peylin, P., Law, R. M., Gurney, K. R., Chevallier, F., Jacobson, A. R., Maki, T., Niwa, Y., Patra, P. K., Peters, W., Rayner, P. J., Rödenbeck, C., van der Laan-Luijkx, I. T., and Zhang, X.: Global atmospheric carbon budget: results from an ensemble of atmospheric CO_2 inversions, Biogeosciences, 10, 6699–6720, https://doi.org/10.5194/bg-10-6699-2013, http://www.biogeosciences.net/10/6699/2013/, 2013.

Piao, S., Sitch, S., Ciais, P., Friedlingstein, P., Peylin, P., Wang, X., Ahlstrom, A., Anav, A., Canadell, J. G., Cong, N., Huntingford, C., Jung, M., Levis, S., Levy, P. E., Li, J., Lin, X., Lomas, M. R., Lu, M., Luo, Y., Ma, Y., Myneni, R. B., Poulter, B., Sun, Z., Wang, T., Viovy, N., Zaehle, S., and Zeng, N.: Evaluation of terrestrial carbon cycle models for their response to climate variability and to CO_2 trends, Global Change Biology, 19, 2117–2132, https://doi.org/10.1111/gcb.12187, http://dx.doi.org/10.1111/gcb.12187, 2013.

Polavarapu, S. M., Neish, M., Tanguay, M., Girard, C., de Grandpré, J., Semeniuk, K., Gravel, S., Ren, S., Roche, S., Chan, D., and Strong, K.: Greenhouse gas simulations with a coupled meteorological and transport model: the predictability of CO_2, Atmospheric Chemistry and Physics, 16, 12 005–12 038, https://doi.org/10.5194/acp-16-12005-2016, http://www.atmos-chem-phys.net/16/12005/2016/, 2016.

Potter, C. S., Randerson, J. T., Field, C. B., Matson, P. A., Vitousek, P. M., Mooney, H. A., and Klooster, S. A.: Terrestrial ecosystem production: a process model based on global satellite and surface data, Global Biogeochemical Cycles, 7, 811–841, 1993.

Rayner, P. J., Scholze, M., Knorr, W., Kaminski, T., Giering, R., and Widmann, H.: Two decades of terrestrial carbon fluxes from a carbon cycle data assimilation system (CCDAS), Global Biogeochemical Cycles, 19, 20 PP., doi:10.1029/2004GB002 254, 2005.

Reichstein, M., Kätterer, T., Andrén, O., Ciais, P., Schulze, E.-D., Cramer, W., Papale, D., and Valentini, R.: Temparature sensitivity of decomposition in relation to soil organic matter pools: critique and outlook, Biogeosciences, 2, 317–321, 2005.

Rienecker, M. M., Suarez, M. J., Gelaro, R., Todling, R., Bacmeister, J., Liu, E., Bosilovich, M. G., Schubert, S. D., Takacs, L., Kim, G.-K., Bloom, S., Chen, J., Collins, D., Conaty, A., da Silva, A., Gu, W., Joiner, J., Koster, R. D., Lucchesi, R., Molod, A., Owens, T., Pawson, S., Pegion, P., Redder, C. R., Reichle, R., Robertson, F. R., Ruddick, A. G., Sienkiewicz, M., and Woollen, J.: MERRA: NASA's Modern-Era Retrospective Analysis for Research and Applications, J. Climate, 24, 3624–3648, https://doi.org/10.1175/JCLI-D-11-00015.1, http://dx.doi.org/10.1175/JCLI-D-11-00015.1, 2011.

Robichaud, A. and Ménard, R.: Multi-year objective analyses of warm season ground-level ozone and $PM_{2.5}$ over North America using real-time observations and Canadian operational air quality models, Atmospheric Chemistry and Physics, 14, 1769–1800, https://doi.org/10.5194/acp-14-1769-2014, http://www.atmos-chem-phys.net/14/1769/2014/, 2014.

Rödenbeck, C., Houweling, S., Gloor, M., and Heimann, M.: CO_2 flux history 1982-2001 inferred from atmospheric data using a global inversion of atmospheric transport, Atmospheric Chemistry and Physics, 3, 1919–1964, 2003.

Scholze, M., Kaplan, J. O., Knorr, W., and Heimann, M.: Climate and interannual variability of the atmosphere-biosphere $13CO_2$ flux, Geophysical Research Letters, 30, 4 PP., doi:10.1029/2002GL015 631, 2003.

Sellers, P. J., Randall, D. A., Collatz, G. J., Berry, J. A., Field, C. B., Dazlich, D. A., Zhang, C., Collelo, C. D., and Bounoua, L.: A revised land surface parameterization (SiB2) for atmospheric GCMs: Part 1. Model formulation, Journal of Climate, 9, 676–705, 1996.

Sherlock, V., Connor, B., Robinson, J., Shiona, H., Smale, D., and Pollard, D.: TCCON data from Lauder, New Zealand, 125HR, Release GGG2014R0, http://dx.doi.org/10.14291/tccon.ggg2014.lauder02.R0/1149298, https://doi.org/10.14291/tccon.ggg2014.lauder02.R0/1149298, TCCON data archive, hosted by the Carbon Dioxide Information Analysis Center, Oak Ridge National Laboratory, Oak Ridge, Tennessee, U.S.A., 2014.

Simmons, A. J., Willett, K. M., Jones, P. D., Thorne, P. W., and Dee, D. P.: Low-frequency variations in surface atmospheric humidity, temperature, and precipitation: Inferences from reanalyses and monthly gridded observational data sets, Journal of Geophysical Research: Atmospheres, 115, https://doi.org/10.1029/2009JD012442, http://dx.doi.org/10.1029/2009JD012442, d01110, 2010.

Sitch, S., Smith, B., Prentice, I. C., Arneth, A., Bondeau, A., Cramer, W., Kaplan, J. O., Levis, S., Lucht, W., Sykes, M. T., Thonicke, K., and Venevsky, S.: Evaluation of ecosystem dynamics, plant geography and terrestrial carbon cycling in the LPJ dynamic global vegetation model, Global Change Biology, 9, 161–185, 2003.

Sitch, S., Friedlingstein, P., Gruber, N., Jones, S. D., Murray-Tortarolo, G., Ahlström, A., Doney, S. C., Graven, H., Heinze, C., Huntingford, C., Levis, S., Levy, P. E., Lomas, M., Poulter, B., Viovy, N., Zaehle, S., Zeng, N., Arneth, A., Bonan, G., Bopp, L., Canadell, J. G., Chevallier, F., Ciais, P., Ellis, R., Gloor, M., Peylin, P., Piao, S. L., Le Quéré, C., Smith, B., Zhu, Z., and Myneni, R.: Recent trends and drivers of regional sources and sinks of carbon dioxide, Biogeosciences, 12, 653–679, https://doi.org/10.5194/bg-12-653-2015, http://www.biogeosciences.net/12/653/2015/, 2015.

Strong, K., Mendonca, J., Weaver, D., Fogal, P., Drummond, J., Batchelor, R., and Lindenmaier, R.: TCCON data from Eureka, Canada, Release GGG2014R0, http://dx.doi.org/10.14291/tccon.ggg2014.eureka01.R0/1149271,

https://doi.org/10.14291/tccon.ggg2014.eureka01.R0/1149271, TCCON data archive, hosted by the Carbon Dioxide Information Analysis Center, Oak Ridge National Laboratory, Oak Ridge, Tennessee, U.S.A., 2014.

Suntharalingam, P., Jacob, D. J., Palmer, P. I., Logan, J. A., Yantosca, R. M., Xiao, Y. P., Evans, M. J., Streets, D. G., Vay, S. L., and Sachse, G. W.: Improved quantification of Chinese carbon fluxes using CO_2/CO correlations in Asian outflow, Journal of Geophysical Research-Atmospheres, 109, D18S18, doi:10.1029/2003JD004 362, 2004.

Sussmann, R. and Rettinger, M.: TCCON data from Garmisch, Germany, Release GGG2014R0, http://dx.doi.org/10.14291/tccon.ggg2014.garmisch01.R0/1149299, https://doi.org/10.14291/tccon.ggg2014.garmisch01.R0/1149299, TCCON data archive, hosted by the Carbon Dioxide Information Analysis Center, Oak Ridge National Laboratory, Oak Ridge, Tennessee, U.S.A., 2014.

Szczypta, C., Calvet, J.-C., Albergel, C., Balsamo, G., Boussetta, S., Carrer, D., Lafont, S., and Meurey, C.: Verification of the new ECMWF ERA-Interim reanalysis over France, Hydrology and Earth System Sciences, 15, 647–666, https://doi.org/10.5194/hess-15-647-2011, http://www.hydrol-earth-syst-sci.net/15/647/2011/, 2011.

Thornton, P. E., Cook, R. B., Braswell, B. H., Law, B. E., Post, W. M., Shugart, H. H., Rhyne, B. T., and Hook, L. A.: Archiving numerical models of biogeochemical dynamics, EOS Transactions, American Geophysical Union, 86, p. 431, 2005.

Tian, H., Lu, C., Yang, J., Banger, K., Huntzinger, D. N., Schwalm, C. R., Michalak, A. M., Cook, R., Ciais, P., Hayes, D., Huang, M., Ito, A., Jain, A. K., Lei, H., Mao, J., Pan, S., Post, W. M., Peng, S., Poulter, B., Ren, W., Ricciuto, D., Schaefer, K., Shi, X., Tao, B., Wang, W., Wei, Y., Yang, Q., Zhang, B., and Zeng, N.: Global patterns and controls of soil organic carbon dynamics as simulated by multiple terrestrial biosphere models: Current status and future directions, Global Biogeochem. Cycles, 29, 775–792, http://dx.doi.org/10.1002/2014GB005021, 2015.

Verseghy, D.: CLASS - the Canadian Land Surface Scheme (Version 3.6), Technical Documentation, Tech. Rep. pp 179, Science and Technology Branch, Environment and Climate Change Canada , Toronto, 2012.

Viovy, N.: CRUNCEP data set version 6, available at: https://vesg.ipsl.upmc.fr/thredds/catalog/store/p529viov/cruncep/V6_1901_2014/catalog.html [last access: June 2016], 2016.

Warneke, T., Messerschmidt, J., Notholt, J., Weinzierl, C., Deutscher, N., Petri, C., Grupe, P., Vuillemin, C., Truong, F., Schmidt, M., Ramonet, M., and Parmentier, E.: TCCON data from Orleans, France, Release GGG2014R0, http://dx.doi.org/10.14291/tccon.ggg2014.orleans01.R0/1149276, https://doi.org/10.14291/tccon.ggg2014.orleans01.R0/1149276, TCCON data archive, hosted by the Carbon Dioxide Information Analysis Center, Oak Ridge National Laboratory, Oak Ridge, Tennessee, U.S.A., 2014.

Wei, Y., Liu, S., Huntzinger, D. N., Michalak, A. M., Viovy, N., Post, W. M., Schwalm, C. R., Schaefer, K., Jacobson, A. R., Lu, C., Tian, H., Ricciuto, D. M., Cook, R. B., Mao, J., and Shi, X.: The North American Carbon Program Multi-scale Synthesis and Terrestrial Model Intercomparison Project - Part 2: Environmental driver data, Geoscientific Model Development, 7, 2875–2893, https://doi.org/10.5194/gmd-7-2875-2014, http://www.geosci-model-dev.net/7/2875/2014/, 2014.

Wennberg, P. O., Roehl, C., Wunch, D., Toon, G. C., Blavier, J.-F., Washenfelder, R., Keppel-Aleks, G., Allen, N., and Ayers, J.: TCCON data from Park Falls, Wisconsin, USA, Release GGG2014R0, http://dx.doi.org/10.14291/tccon.ggg2014.parkfalls01.R0/1149161, https://doi.org/10.14291/tccon.ggg2014.parkfalls01.R0/1149161, TCCON data archive, hosted by the Carbon Dioxide Information Analysis Center, Oak Ridge National Laboratory, Oak Ridge, Tennessee, U.S.A., 2014a.

Wennberg, P. O., Wunch, D., Roehl, C., Blavier, J.-F., Toon, G. C., Allen, N., Dowell, P., Teske, K., Martin, C., and Martin., J.: TCCON data from Lamont, Oklahoma, USA, Release GGG2014R0, http://dx.doi.org/10.14291/tccon.ggg2014.lamont01.R0/1149159,

https://doi.org/10.14291/tccon.ggg2014.lamont01.R0/1149159, TCCON data archive, hosted by the Carbon Dioxide Information Analysis Center, Oak Ridge National Laboratory, Oak Ridge, Tennessee, U.S.A., 2014b.

Wofsy, S., Daube, B., Jimenez, R., Kort, E., Pittman, J., Park, S., Commane, R., Xiang, B., Santoni, G., Jacob, D., Fisher, J., Pickett-Heaps, C., Wang, H., Wecht, K., Wang, Q.-Q., Stephens, B., Shertz, S., Watt, A., Romashkin, P., Campos, T., Haggerty, J., Cooper, W., Rogers, D., Beaton, S., Hendershot, R., Elkins, J., Fahey, D., Gao, R., Moore, F., Montzka, S., Schwarz, J., Perring, A., Hurst, D., Miller, B., Sweeney, C., Oltmans, S., Nance, D., Hintsa, E., Dutton, G., Watts, L., Spackman, J., Rosenlof, K., Ray, E., Hall, B., Zondlo, M., Diao, M., Keeling, R., Bent, J., Atlas, E., Lueb, R., and Mahoney, M.: HIPPO Merged 10-second Meteorology, Atmospheric Chemistry, and Aerosol Data (R20121129), https://doi.org/10.3334/cdiac/hippo_010, 2012.

Wofsy, S. C.: HIAPER Pole-to-Pole Observations (HIPPO): fine-grained, global-scale measurements of climatically important atmospheric gases and aerosols, Philosophical Transactions of the Royal Society of London A: Mathematical, Physical and Engineering Sciences, 369, 2073–2086, 2011.

Worthy, D. E. J., Chan, E., Ishizawa, M., Chan, D., Poss, C., Dlugokencky, E. J., Maksyutov, S., and Levin, I.: Decreasing anthropogenic methane emissions in Europe and Siberia inferred from continuous carbon dioxide and methane observations at Alert, Canada, Journal of Geophysical Research: Atmospheres, 114, https://doi.org/10.1029/2008JD011239, http://dx.doi.org/10.1029/2008JD011239, d10301, 2009.

Wunch, D., Toon, G. C., Blavier, J.-F. L., Washenfelder, R. A., Notholt, J., Connor, B. J., Griffith, D. W., Sherlock, V., and Wennberg, P. O.: The total carbon column observing network, Philosophical Transactions of the Royal Society of London A: Mathematical, Physical and Engineering Sciences, 369, 2087–2112, 2011.

Wutzler, T. and Reichstein, M.: Soils apart from equilibrium – consequences for soil carbon balance modelling, Biogeosciences, 4, 125–136, https://doi.org/10.5194/bg-4-125-2007, http://www.biogeosciences.net/4/125/2007/, 2007.

Yokota, T., Yoshida, Y., Eguchi, N., Ota, Y., Tanaka, T., Watanabe, H., and Maksyutov, S.: Global Concentrations of CO_2 and CH_4 Retrieved from GOSAT: First Preliminary Results, SOLA, 5, 160–163, https://doi.org/10.2151/sola.2009-041, 2009.

Zhao, M., Running, S. W., and Nemani, R. R.: Sensitivity of Moderate Resolution Imaging Spectroradiometer (MODIS) terrestrial primary production to the accuracy of meteorological reanalyses, J. Geophys. Res., 111, http://dx.doi.org/10.1029/2004JG000004, 2006.

Zhu, Q. and Zhuang, Q.: Ecosystem biogeochemistry model parameterization: Do more flux data result in a better model in predicting carbon flux?, Ecosphere, 6, 1–20, https://doi.org/10.1890/ES15-00259.1, http://dx.doi.org/10.1890/ES15-00259.1, 2015.

Zobler, L.: A World Soil File for Global Climate Modelling. NASA Technical Memorandum 87802, http://daac.ornl.gov/SOILS/guides/ZoblerSoil1.html, 1986.

Geosci. Model Dev. Discuss., https://doi.org/10.5194/gmd-2017-169
Manuscript under review for journal Geosci. Model Dev.
Discussion started: 11 September 2017

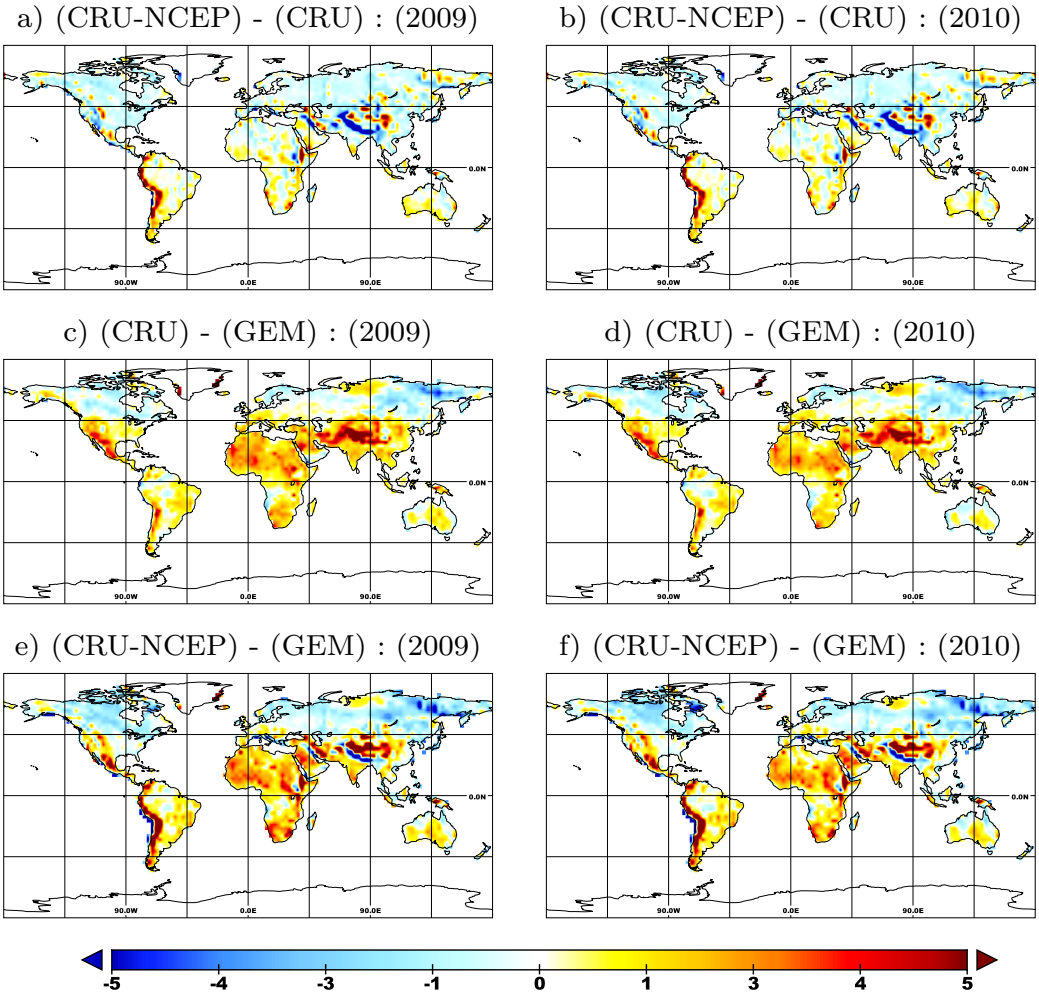

Figure 1. Comparison of spatial distribution patterns of annual mean temperature (°C) for 2009 and 2010: (a and b) CRU-NCEP minus CRU, (c and d) CRU minus GEM , and (e and f) CRU-NCEP minus GEM.

Geosci. Model Dev. Discuss., https://doi.org/10.5194/gmd-2017-169
Manuscript under review for journal Geosci. Model Dev.
Discussion started: 11 September 2017

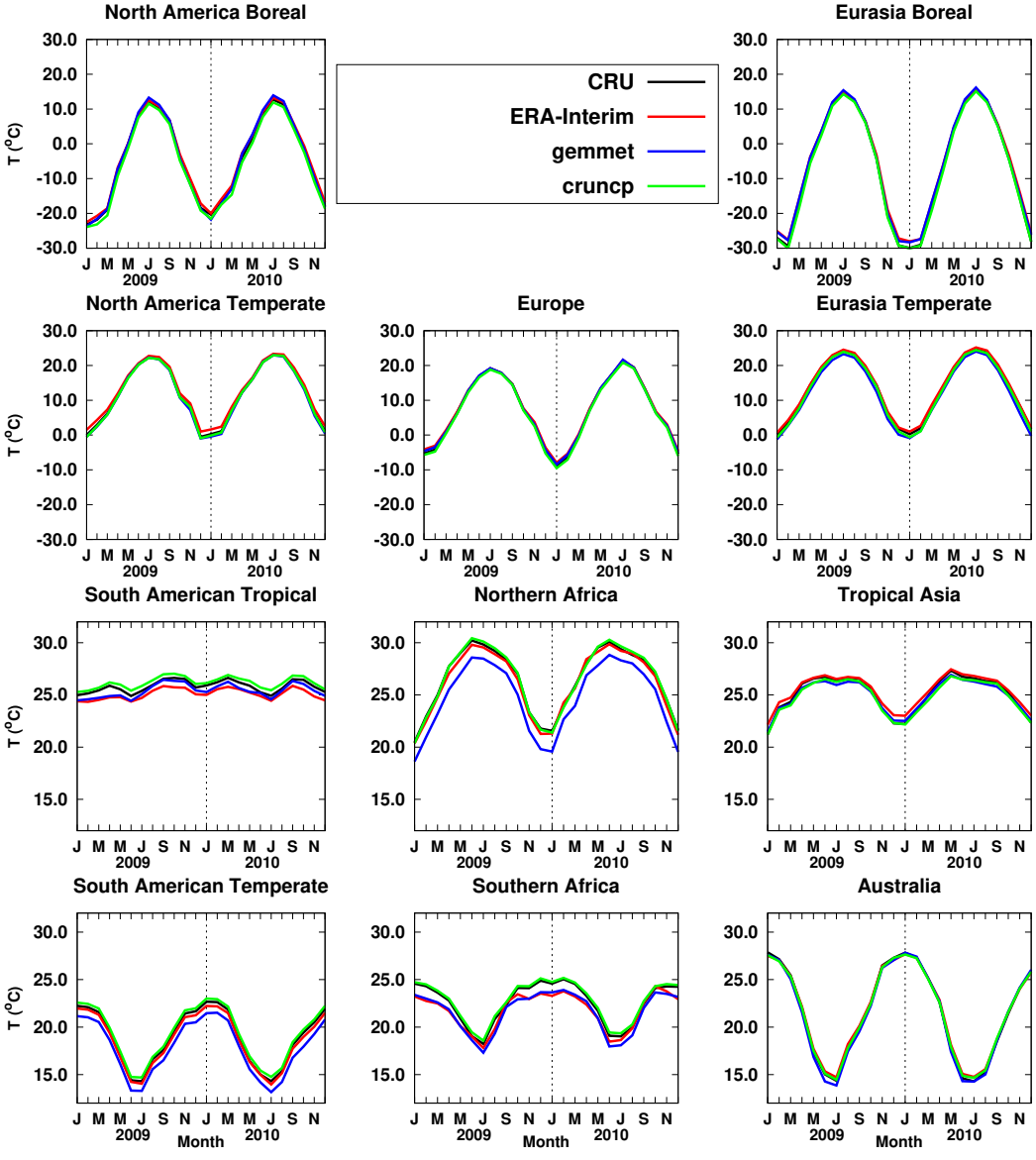

Figure 2. Monthly mean temperature (°C) averaged for the TransCom land regions.

Geosci. Model Dev. Discuss., https://doi.org/10.5194/gmd-2017-169
Manuscript under review for journal Geosci. Model Dev.
Discussion started: 11 September 2017

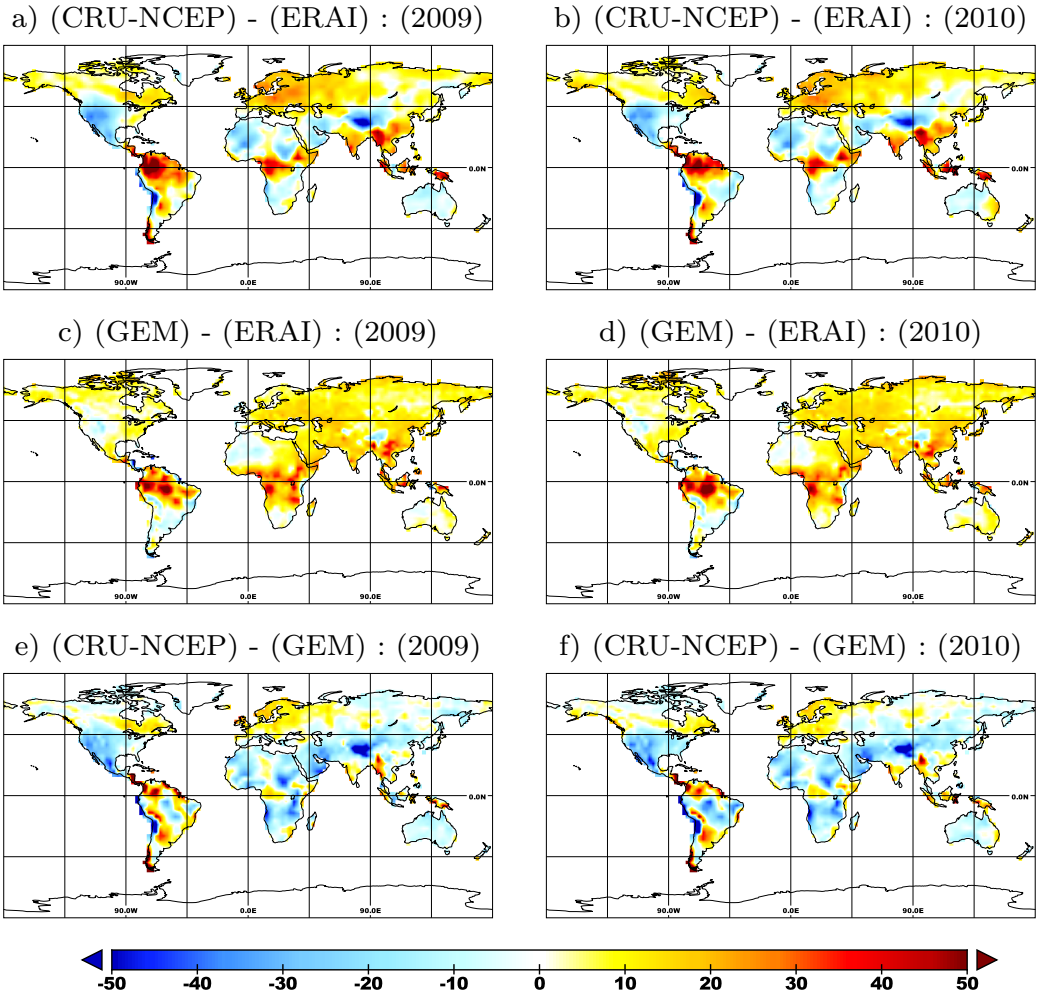

Figure 3. Comparison of spatial distribution patterns of annual mean shortwave radiation (W m^{-2}) for 2009 and 2010: (a and b) CRU-NCEP minus ERAI, (c and d) GEM minus ERAI, and (e and f) CRU-NCEP minus GEM.

Geosci. Model Dev. Discuss., https://doi.org/10.5194/gmd-2017-169
Manuscript under review for journal Geosci. Model Dev.
Discussion started: 11 September 2017

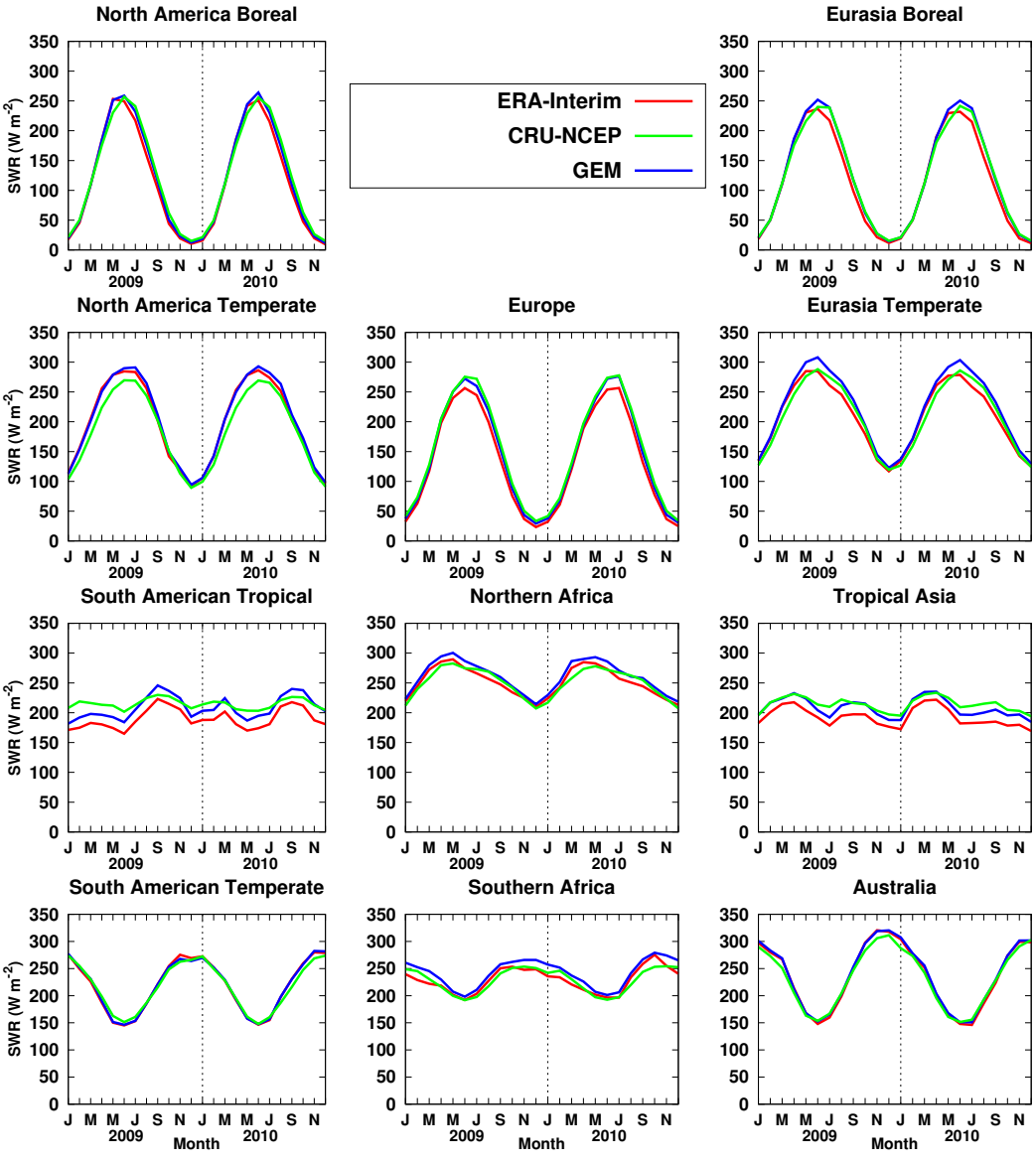

Figure 4. Monthly mean shortwave radiation (W m^{-2}) averaged for the 11 TransCom land regions.

Geosci. Model Dev. Discuss., https://doi.org/10.5194/gmd-2017-169
Manuscript under review for journal Geosci. Model Dev.
Discussion started: 11 September 2017

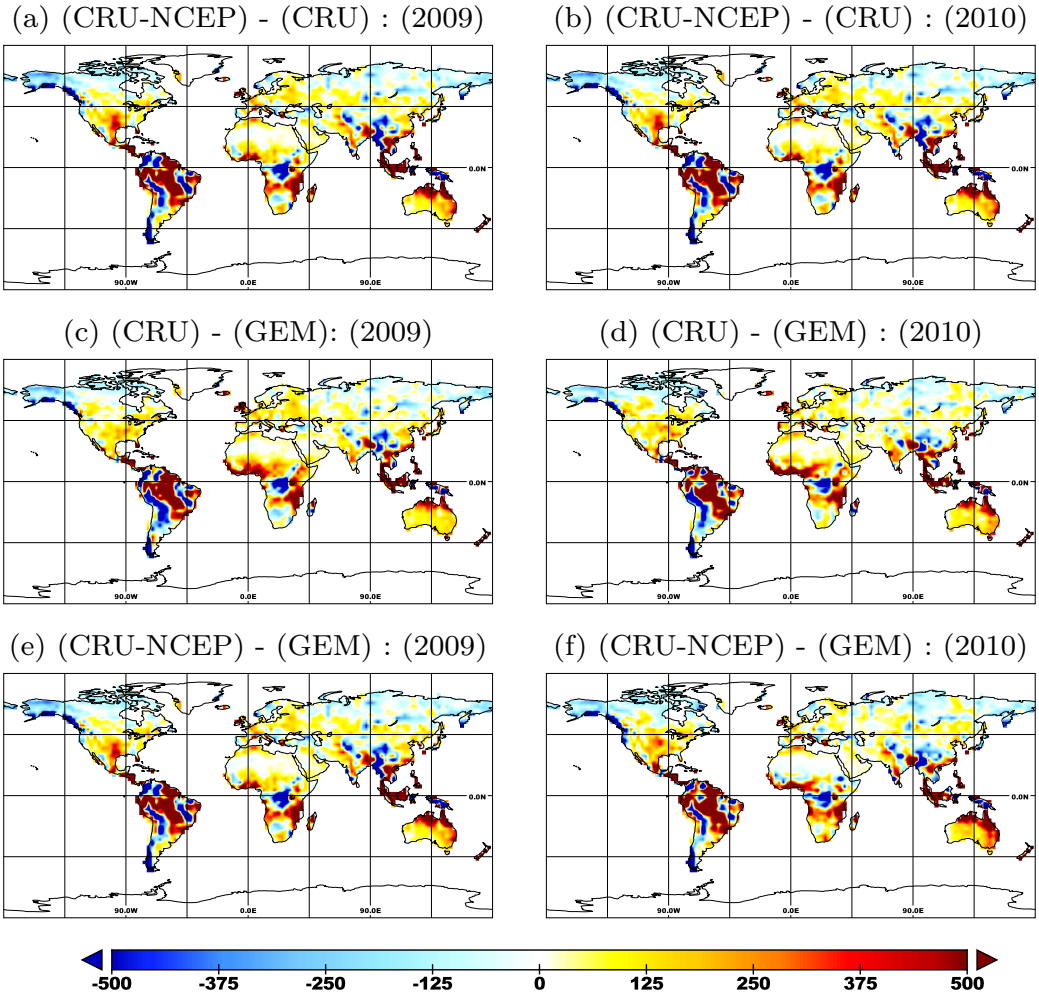

Figure 5. Comparison of spatial distribution patterns of annual total precipitation (mm year^{-1}) for 2009 and 2010: (a) and (b) CRU-NCEP minus CRU, (c) and (d) CRU minus GEM, and (e) and (f) CRU-NCEP minus GEM.

Geosci. Model Dev. Discuss., https://doi.org/10.5194/gmd-2017-169
Manuscript under review for journal Geosci. Model Dev.
Discussion started: 11 September 2017

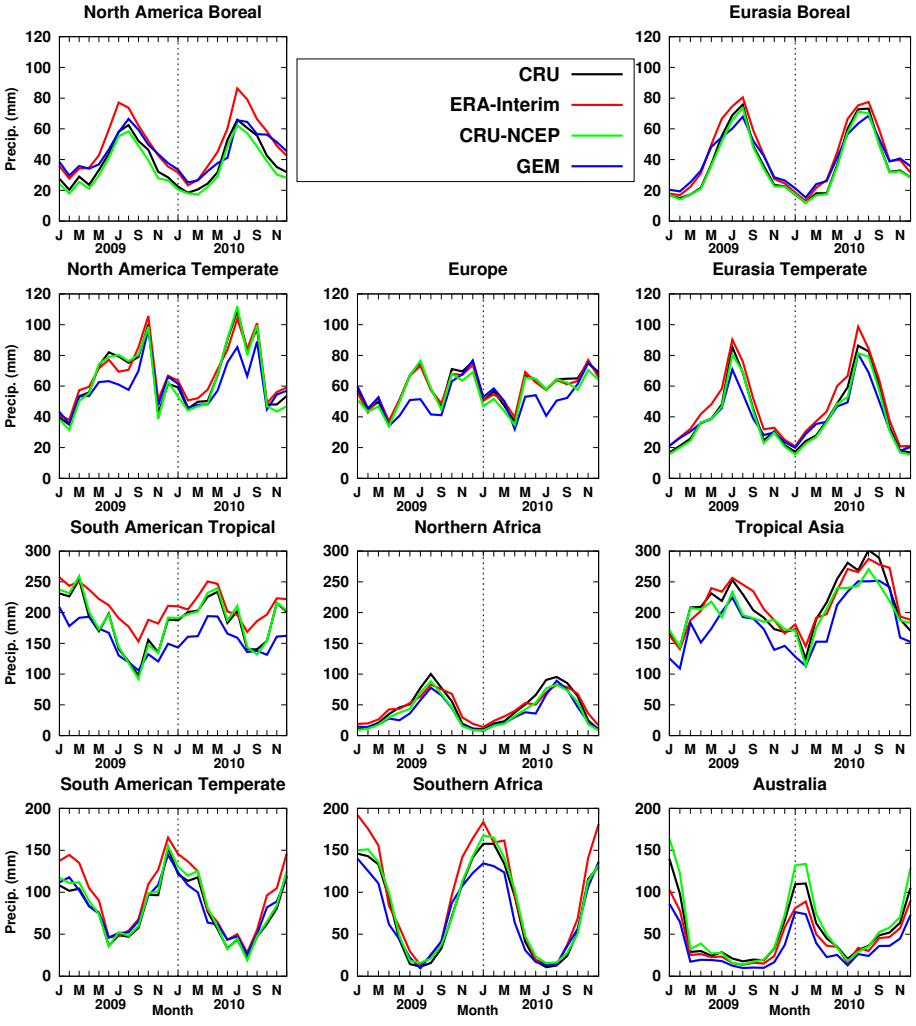

Figure 6. Monthly total precipitation (mm month^{-1}) for the 11 TransCom land regions.

Geosci. Model Dev. Discuss., https://doi.org/10.5194/gmd-2017-169
Manuscript under review for journal Geosci. Model Dev.
Discussion started: 11 September 2017

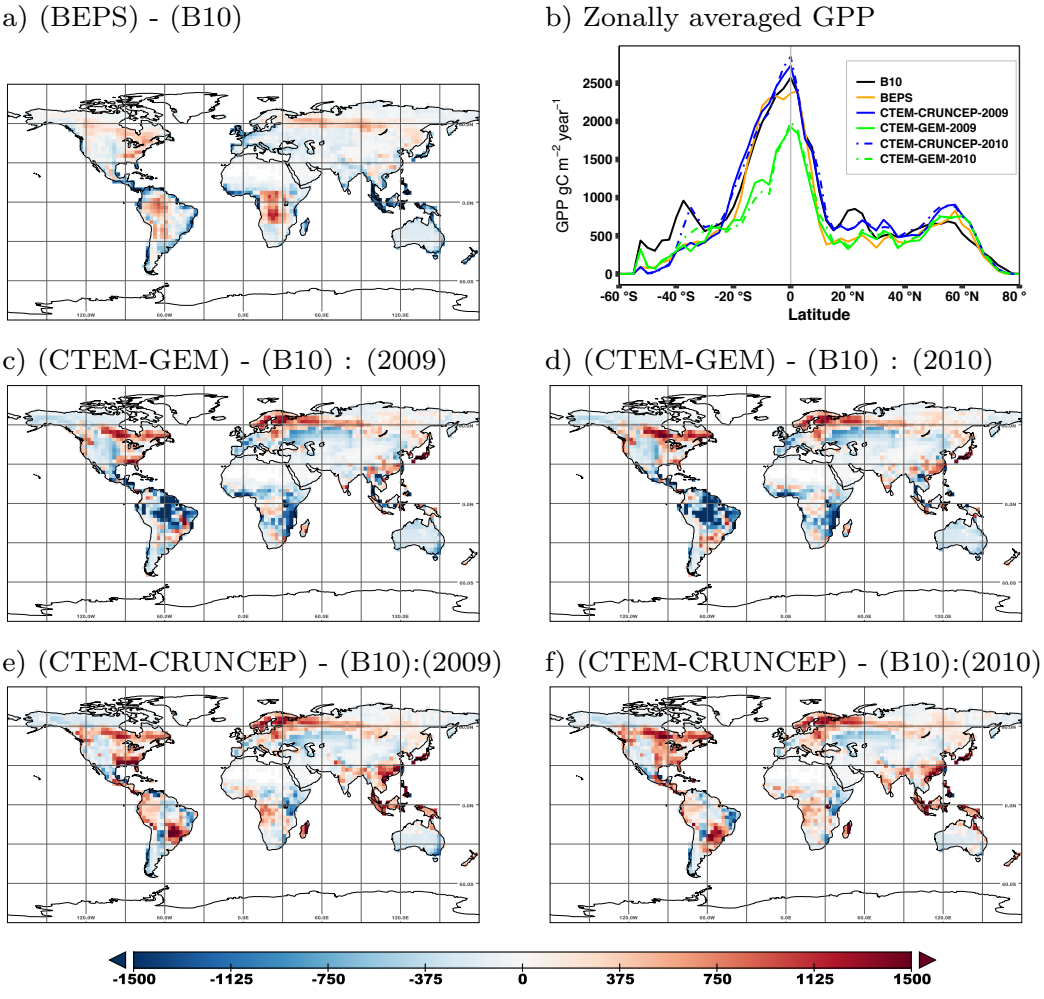

Figure 7. The annual spatial difference of GPP (gC m^{-2} $year^{-1}$) for CTEM-GEM, CTEM-CRUNCEP, and BEPS for 2009 and 2010 against the observation-based GPP estimates from B10 (averaged over the period 1998 to 2005). The zonal distributions of GPP from all datasets are shown (top-right).

Geosci. Model Dev. Discuss., https://doi.org/10.5194/gmd-2017-169
Manuscript under review for journal Geosci. Model Dev.
Discussion started: 11 September 2017

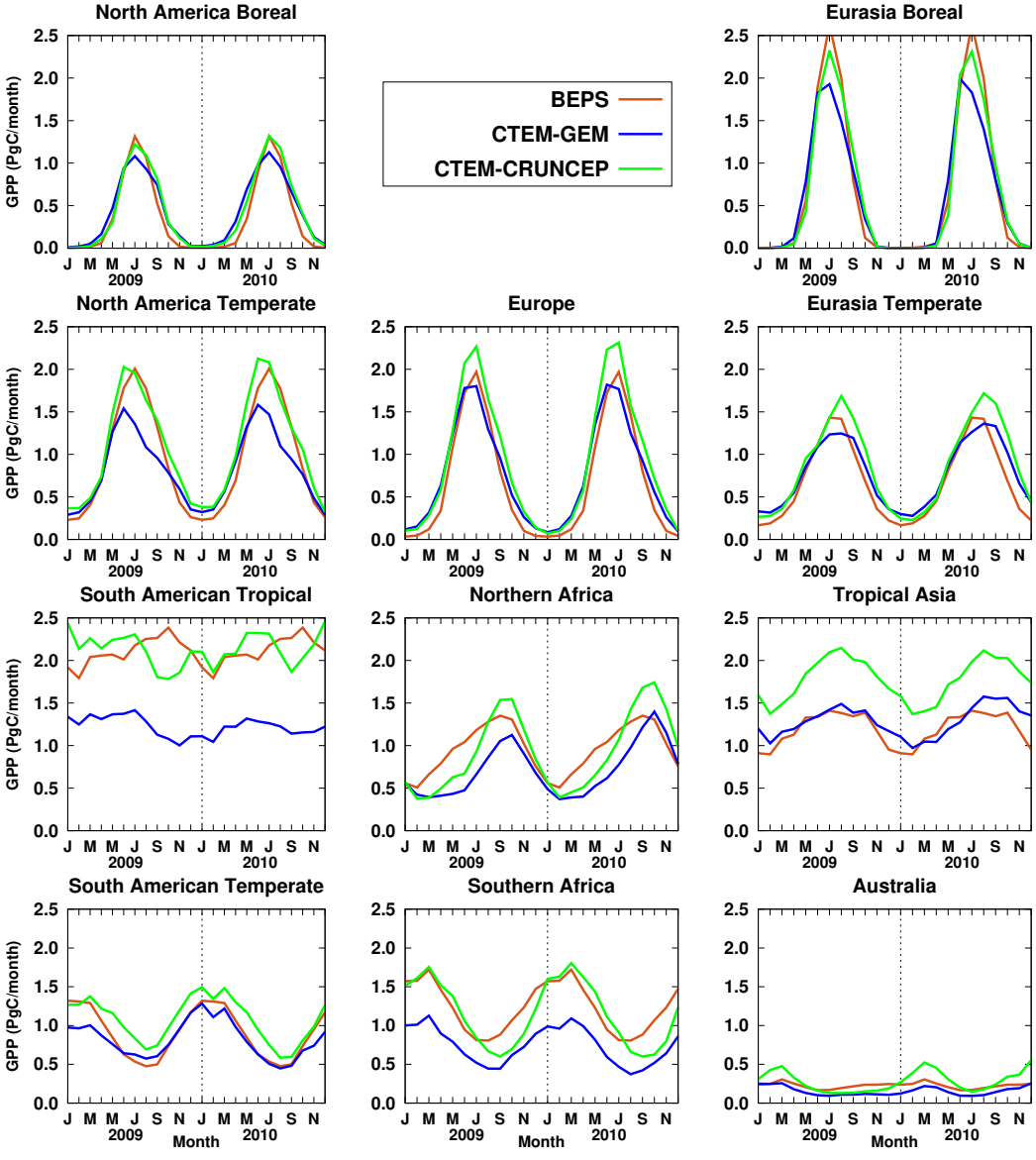

Figure 8. The seasonal cycle of GPP from CTEM-GEM, CTEM-CRUNCEP, and BEPS integrated over the 11 TransCom land regions.

Geosci. Model Dev. Discuss., https://doi.org/10.5194/gmd-2017-169
Manuscript under review for journal Geosci. Model Dev.
Discussion started: 11 September 2017

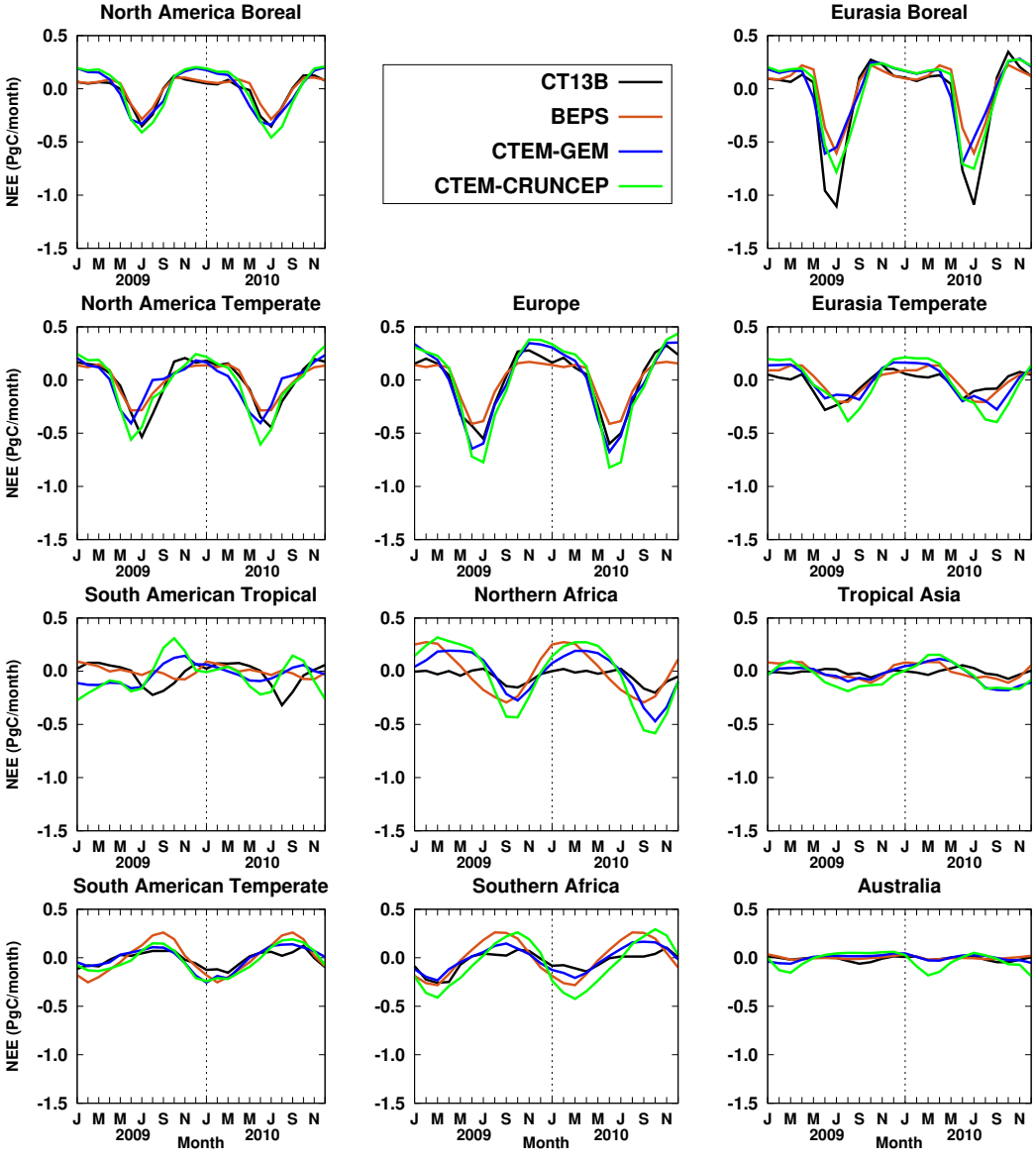

Figure 9. The seasonal cycle of NEE from CTEM-GEM, CTEM-CRUNCEP, and BEPS in comparison to the optimized NEE from CT2013B integrated over the 11 TransCom land regions.

Geosci. Model Dev. Discuss., https://doi.org/10.5194/gmd-2017-169
Manuscript under review for journal Geosci. Model Dev.
Discussion started: 11 September 2017

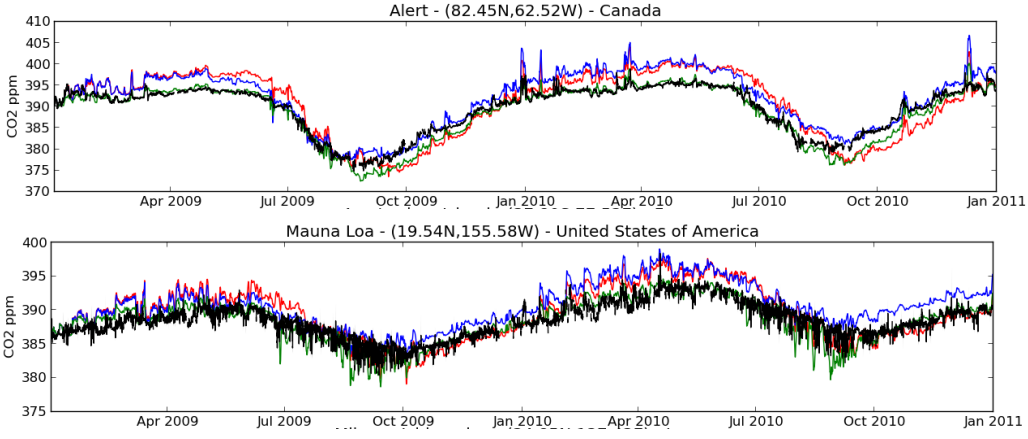

Figure 10. Comparison of modelled CO_2 using land prior fluxes from CTEM-CRUNCEP (red) and CTEM-GEM (blue) with surface observations (black) at Alert (top), and Mauna Loa (bottom), and modelled CO_2 using posterior fluxes from CT2013B (green). The modelled CO_2 was produced by a forward run of GEM-MACH-GHG.

Geosci. Model Dev. Discuss., https://doi.org/10.5194/gmd-2017-169
Manuscript under review for journal Geosci. Model Dev.
Discussion started: 11 September 2017

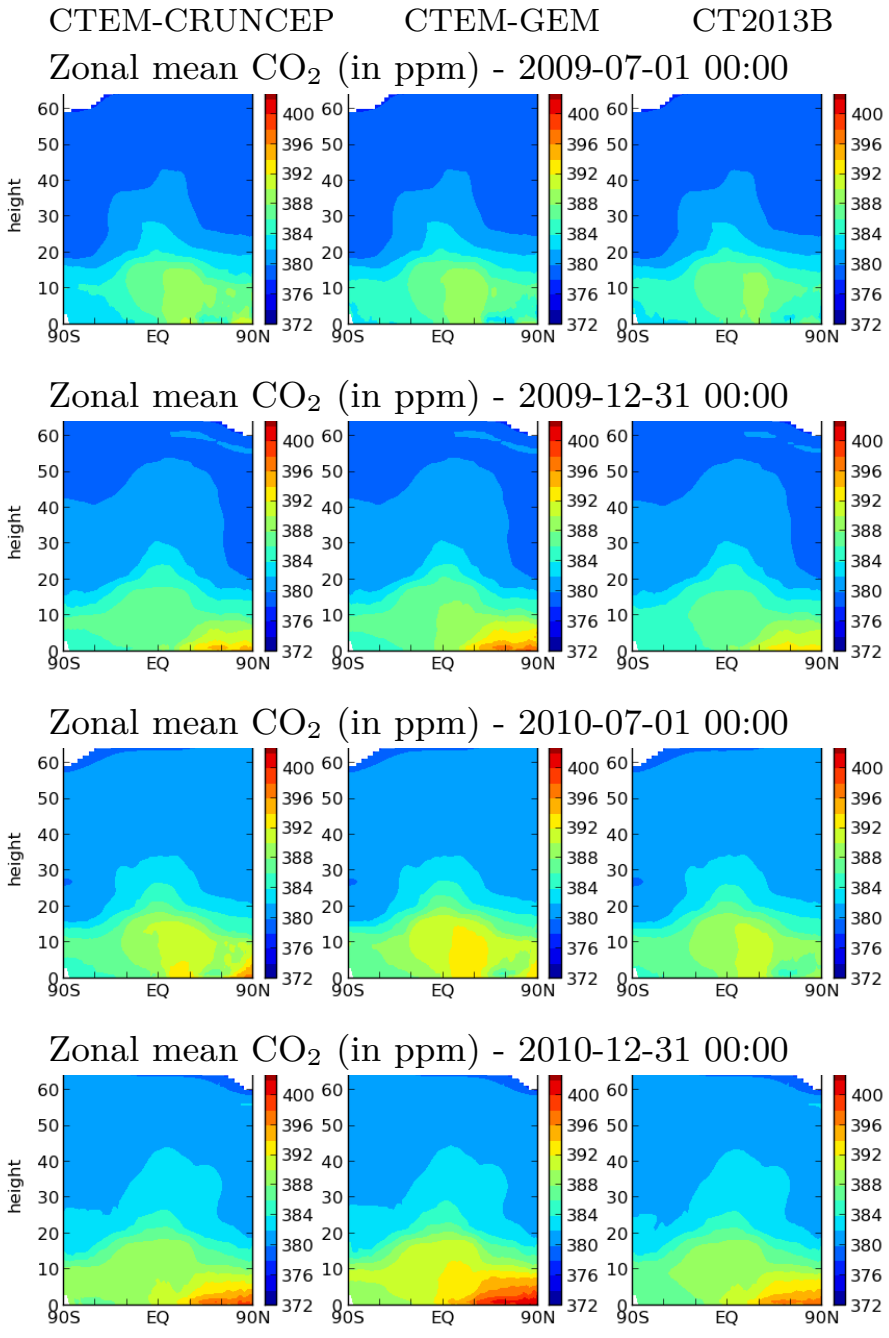

Figure 11. Zonal mean CO_2 on 1 July 2009 and 31 Dec. 2010 (top two rows), and 1 July 2009 and 31 Dec. 2010(bottom two row) for CTEM-CRUNCEP (left column), CTEM-GEM (middle column), and CT2013B (right column). The modelled CO_2 was produced by a forward run of GEM-MACH-GHG.

Geosci. Model Dev. Discuss., https://doi.org/10.5194/gmd-2017-169
Manuscript under review for journal Geosci. Model Dev.
Discussion started: 11 September 2017

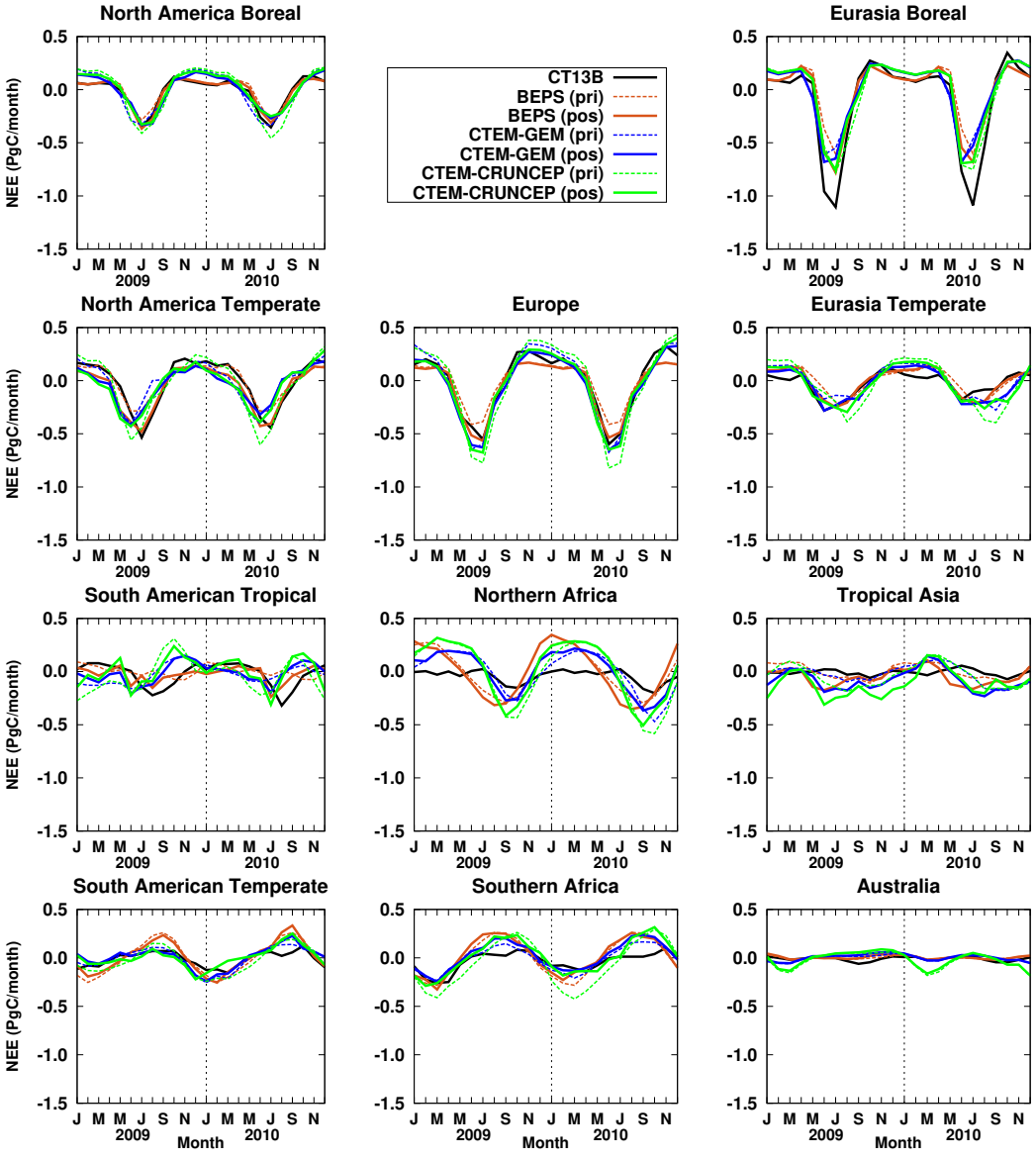

Figure 12. The The seasonal cycle of the optimized NEE from GEOS-Chem using three different prior estimates of NEE from CTEM-GEM, CTEM-CRUNCEP, and BEPS (indicated as well) in comparison to the the optimized NEE from CT2013B integrated over the 11 TransCom land regions.

Geosci. Model Dev. Discuss., https://doi.org/10.5194/gmd-2017-169
Manuscript under review for journal Geosci. Model Dev.
Discussion started: 11 September 2017

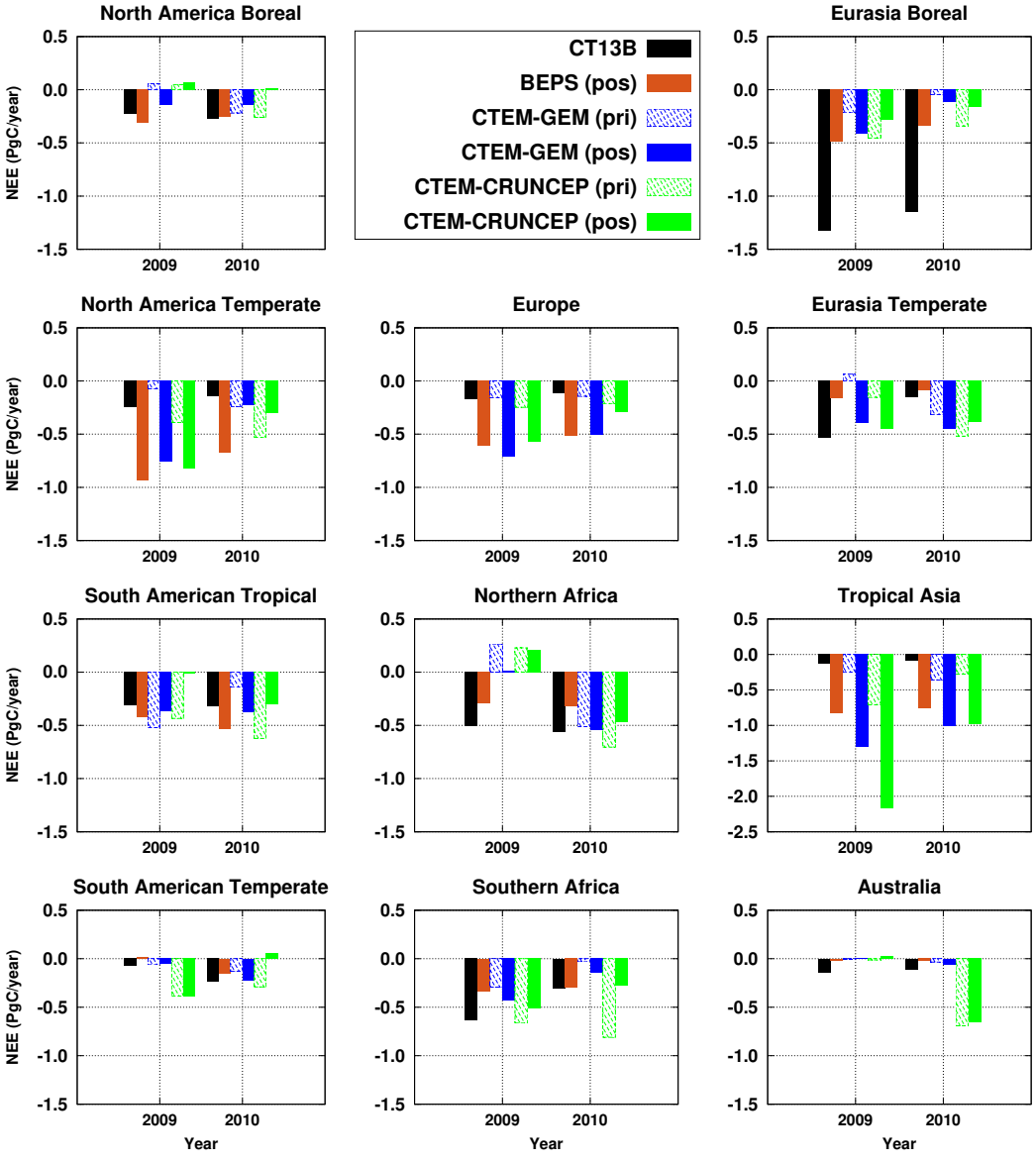

Figure 13. The annual total of the optimized NEE from GEOS-Chem using three different prior flux estimates of NEE from CTEM-GEM, CTEM-CRUNCEP, and BEPS (indicated as well) in comparison to the the optimized NEE from CT2013B integrated over the 11 TransCom land regions.

Geosci. Model Dev. Discuss., https://doi.org/10.5194/gmd-2017-169
Manuscript under review for journal Geosci. Model Dev.
Discussion started: 11 September 2017

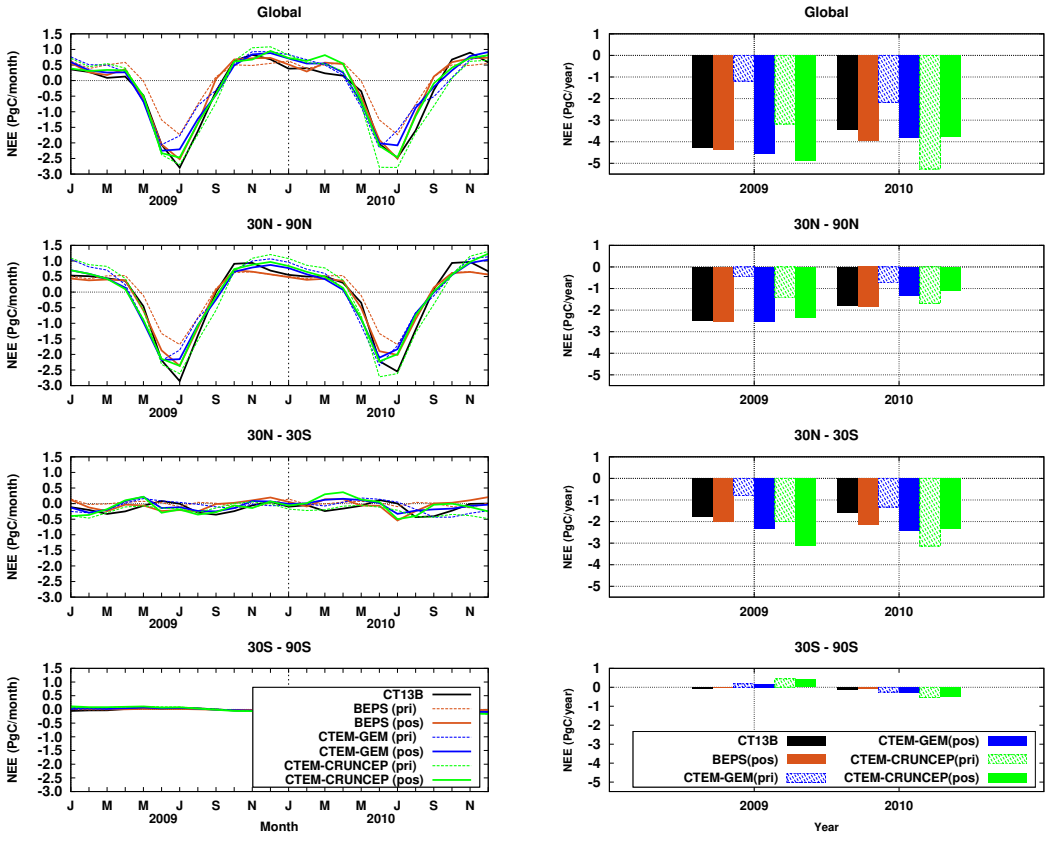

Figure 14. The monthly (left) and annual total (right) of the optimized NEE from GEOS-Chem using three different prior flux estimates of NEE from CTEM-GEM, CTEM-CRUNCEP, and BEPS (indicated as well) in comparison to the the optimized NEE from CT2013B integrated over three latitudinal bands.

Geosci. Model Dev. Discuss., https://doi.org/10.5194/gmd-2017-169
Manuscript under review for journal Geosci. Model Dev.
Discussion started: 11 September 2017

Geoscientific Model Development Discussions
Open Access
EGU

Table 1. TCCON sites used in this study.

Site Name	Lat	Lon	Reference
Eureka, Canada	80.05 N	86.42 W	Strong et al. (2014)
Sodankyla, Finland	67.37 N	26.63 E	Kivi et al. (2014)
Bialystok, Poland	53.23 N	23.03 E	Deutscher et al. (2014)
Bremen, Germany	53.10 N	8.85 E	Notholt et al. (2014)
Karlsruhe, Germany	49.10 N	8.44 E	Hase et al. (2014)
Orleans, France	47.97 N	2.11 E	Warneke et al. (2014)
Garmisch, Germany	47.48 N	11.06 E	Sussmann and Rettinger (2014)
Park Falls, USA	45.95 N	90.27 W	Wennberg et al. (2014a)
Lamont, USA	36.60 N	97.49 W	Wennberg et al. (2014b)
Izana, Tenerife, Spain	28.3 N	16.5 W	Blumenstock et al. (2014)
Darwin, Australia	12.42 S	130.90 E	Griffith et al. (2014a)
Wollongong, Australia	34.41 S	150.88 E	Griffith et al. (2014b)
Lauder, New Zealand	45.04 S	169.68 E	Sherlock et al. (2014)

Table 2. Simulated global values of primary carbon pools and fluxes for the spin-up simulations using CTEM-CRUNCEP, CTEM-GEM and CTEM-CRUNCEP2yr. Values are a 20 year average at the end of model simulations. Mean areal precipitation (global land and for the 30°N-30°S land band) averaged for the 1901-1940 period used to spin-up CTEM-CRUNCEP, and for the 2009-2010 period used to spin-up CTEM-GEM and CTEM-CRUNCEP2yr, and the correspondence GPP estimates.

Variable	CTEM-CRUNCEP	CTEM-GEM	CTEM-CRUNCEP2yr
Gross primary productivity (Pg C yr^{-1})	118.0	97.0	139.8
Net primary productivity (Pg C yr^{-1})	58.0	47.0	70.0
Autotrophic respiration (Pg C yr^{-1})	60.5	49.6	69.8
Heterotrophic respiration (Pg C yr^{-1})	57.5	47.4	70.0
Litter carbon respiration (Pg C yr^{-1})	40.8	33.4	49.4
Soil carbon respiration (Pg C yr^{-1})	16.7	13.7	20.5
Vegetation biomass (Pg C)	674.0	544.0	829.2
Litter mass (Pg C)	97.0	79.0	108.9
Soil carbon mass (Pg C)	1410.0	1162.0	1843.0
Mean areal precipitation (mm yr^{-1}) (global)	760.0	762.0	828.0
Mean areal precipitation (mm yr^{-1}) (30°N-30°S)	1047.0	984.0	1139.0
Gross primary productivity (Pg C yr^{-1}) (30°N-30°S)	80.7	60.9	95.5

Geosci. Model Dev. Discuss., https://doi.org/10.5194/gmd-2017-169
Manuscript under review for journal Geosci. Model Dev.
Discussion started: 11 September 2017

Geoscientific Model Development Discussions
Open Access
EGU

Table 3. Annual GPP, R_{eco}, and NEE (Pg C year^{-1}) from CTEM-CRUNCEP and CTEM-GEM for the transient simulations. The transient simulation was initialized from the spin-up simulations using varying CO_2 concentrations and meteorology.

	CTEM-CRUNCEP		CTEM-GEM		other estimates
	2009	2010	2009	2010	multi-year average
GPP	133.6	137.4	99.3	100.9	119.5 (Deng et al., 2014)
					123 ±8 (Beer et al., 2010)
R_{eco}	130.4	132.2	98.1	98.7	
NEE	-3.2	-5.2	-1.2	-2.2	

Table 4. The mean differences and RMSEs (in ppm) of the a posteriori CO_2 fields, based on CTEM-CRUNCEP, CTEM-GEM, and BEPS fluxes, with respect to TCCON data in 2009 and 2010.

	Mean (mod − obs)			RMSE (mod − obs)		
	CTEM-CRUNCEP	CTEM-GEM	BEPS	CTEM-CRUNCEP	CTEM-GEM	BEPS
2009	0.13	0.27	0.50	1.42	1.24	1.22
2010	0.78	0.80	0.54	1.42	1.39	1.18

Table 5. The mean differences and RMSEs (in ppm) of the a posteriori CO_2 fields, based on CTEM-CRUNCEP, CTEM-GEM, and BEPS fluxes, with respect to aircraft data from the HIPPO-1, HIPPO-2, and HIPPO-3 campaigns.

	Mean (mod − obs)			RMSE (mod − obs)		
	CTEM-CRUNCEP	CTEM-GEM	BEPS	CTEM-CRUNCEP	CTEM-GEM	BEPS
HIPPO-1	-0.01	-0.11	-0.20	2.85	2.65	1.90
HIPPO-2	-0.69	-0.67	-0.41	1.84	1.77	1.55
HIPPO-3	0.26	0.16	-0.28	1.04	0.94	0.87